ELEKTRISCHE DRUCKSONDIERUNGEN

STANDORTCHARAKTERISIERUNG
STARKBEBENSTATION RENNAZ
PARZELLE NR 157, PRAZ-RIOND 8
1847 RENNAZ

Projekt Nr.: 60-748
Band 1 von 1

Geoprofile GmbH

ELEKTRISCHE DRUCKSONDIERUNGEN
STANDORTCHARAKTERISIERUNG STARKBEBENSTATION RENNAZ
PARZELLE NR 157, PRAZ-RIOND 8
1847 RENNAZ

Bauherrschaft	Schweizerische Erdbebendienst SED
Auftraggeber	Schweizerische Erdbebendienst SED
Adresse	Sonneggstrasse 5 8092 Zürich Hr. Walter Imperatori
Referenz Nr. des Auftraggebers	-
Projekt Nr. Geoprofile GmbH	**60-748**
Band	1 von 1
Vertraulichkeit	Verteilung des Berichts beschränkt auf vom Auftraggeber genehmigten Projektteilnehmer

Kurzbeschreibung

Die Bauherrschaft betreibt an der Brühlstrasse 120 auf der Parzelle GB 2029 in 4500 Solothurn eine Messanlage für Starkerdbeben (Bezeichnung SOLB).

Zwecks einer erweiterten Charakterisierung der lokalen Untergrundverhältnisse wurde Geoprofile GmbH vom Auftraggeber beauftragt, eine elektrische Drucksondierung abzuteufen.

Der vorliegende Bericht dokumentiert die folgenden geotechnischen Leistungen:

- Abteufen von 3 elektrische Drucksondierung mit einer Länge von insgesamt 90.0 m (CPTU1 – CPTU3);
- Messung der Laufzeit zwischen einer an der Oberfläche eingeleiteten Scherwelle und dem Geophon in verschiedenen Tiefen (CPTU2);
- Auswertung der Messdaten;
- Geotechnische Interpretation der elektrischen Drucksondierungen und Herleitung von geotechnischen Kennwerten;
- Bestimmung der Scherwellengeschwindigkeit als Funktion der Tiefe;

Feldarbeiten: 21. April 2016

Version	Datum	Beschreibung	Kontrolliert	Genehmigt
1	13.06.2016	Vorabzug Schlussbericht	bshs	hjt

INHALTSVERZEICHNIS Seite

BEILAGEN

ANHÄNGE (allgemeine Hintergrundinformationen)

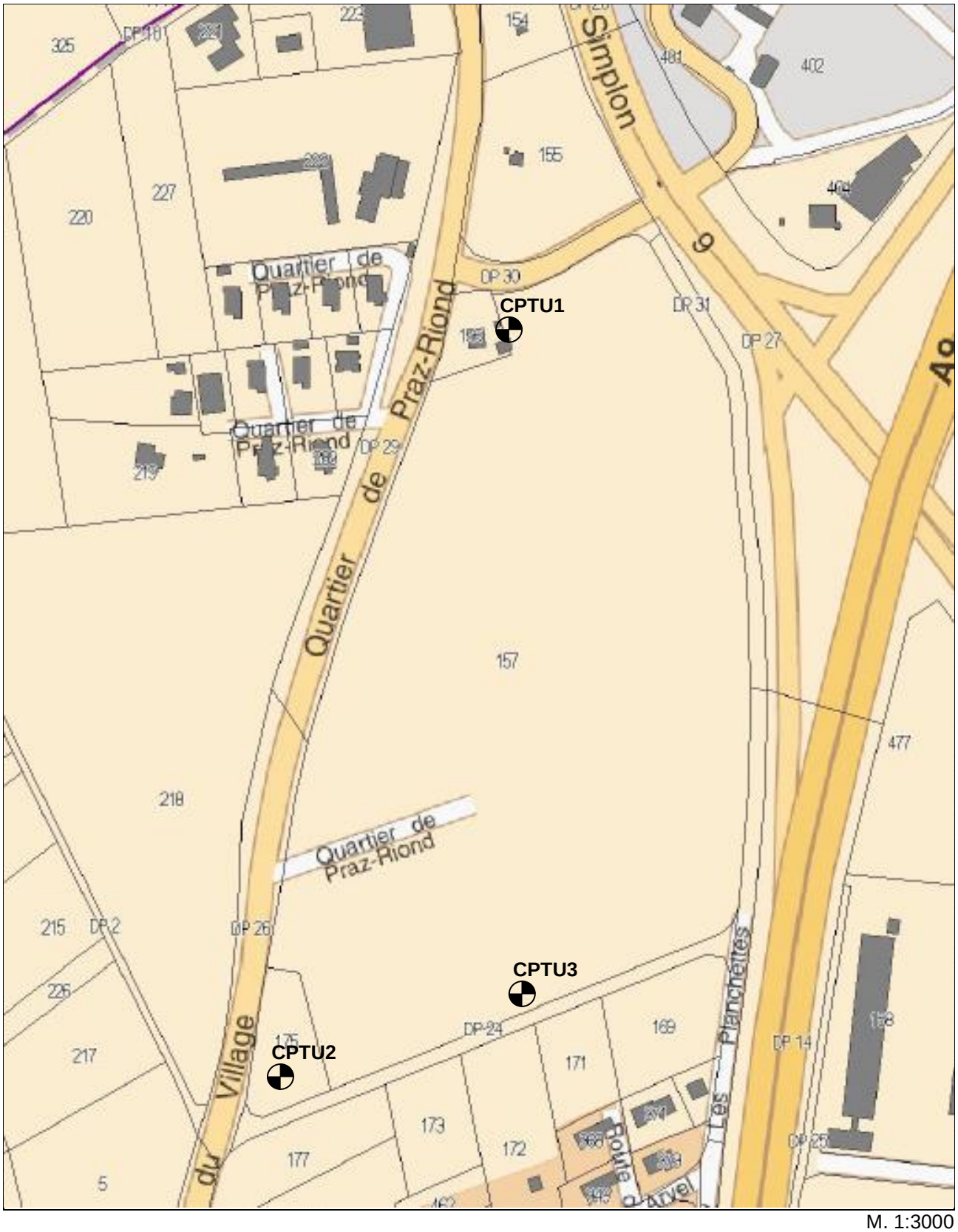

M. 1:3000

SITUATION MIT LAGE DER SONDIERSTELLEN

Standortcharakterisierung Starkbebenstation Rennaz, Parzelle Nr. 157, 1847 Rennaz

BEILAGE A

AUSFÜHRUNGSPRAXIS

INHALT Beilage

TESTSTEUERUNG – PENETRATION

Generelle Testablauf:	Siehe Anhang 1, “elektrische Drucksondierung (CPT)” (GEO/APP/001)
Vorbereitungsphase:	– Bestimmung der Sondierstandorte durch Auftraggeber – Auswahl der Messsonde durch Geoprofile GmbH – Vorherige Sättigung des Filter-Elementes durch Vakuum-Lagerung in Sonnenblumen-Öl während 24 Stunden – Nachsättigung vor Ort vor jeder Prüfung
Einmessen und Nivellement:	– Einmessen der Sondierstandorte durch Auftraggeber – Nivellement durch Auftraggeber
Testphase:	Keine projektspezifischen Vorkehrungen
Testabbruch:	Siehe Anhang 1, “elektrische Drucksondierung (CPT)” (GEO/APP/001)
Zusätzliche Messungen:	Seismische Sondierung CPTU2
Vorbohren:	-

SONDIERGERÄT

Schubvorrichtung:	Hydraulische Schubeinheit mit einem maximalen Druck von 150 kN und einem Hub von 1 m
Aufbau der Schubvorrichtung:	Allein stehend
Reaktionsmasse:	Sondierlastwagen 18to
Schubgestänge:	36 mm A.D.
Schutzverrohrung:	Nicht zutreffend
Reibungsminderer:	Integriert in der Messsonde
Penetrometer:	– Typ S15CFIIP15 – Unabhängige Messung des Spitzenwiderstands q_c, lokale Mantelreibung f_s, Porenwasserüberdruck u_2, Abweichung von der Vertikale in X- und Y-Richtung (i_x und i_y) – Spitzenquerschnitt 15 cm^2 – Oberfläche des Reibungsmantels 225 cm^2 – Netto Flächenverhältnis a: 0.85

DATENAUFZEICHNUNG UND -BEARBEITUNG

Datenaufzeichnung:	Digitale Aufzeichnung, 1 Messung pro cm Eindringung
Tiefenkorrektur:	Korrektion der Sondiertiefe für der Abweichung von der Vertikale

BEILAGE B

ELEKTRISCHE DRUCKSONDIERUNG - MESSDATEN

INHALT Beilage

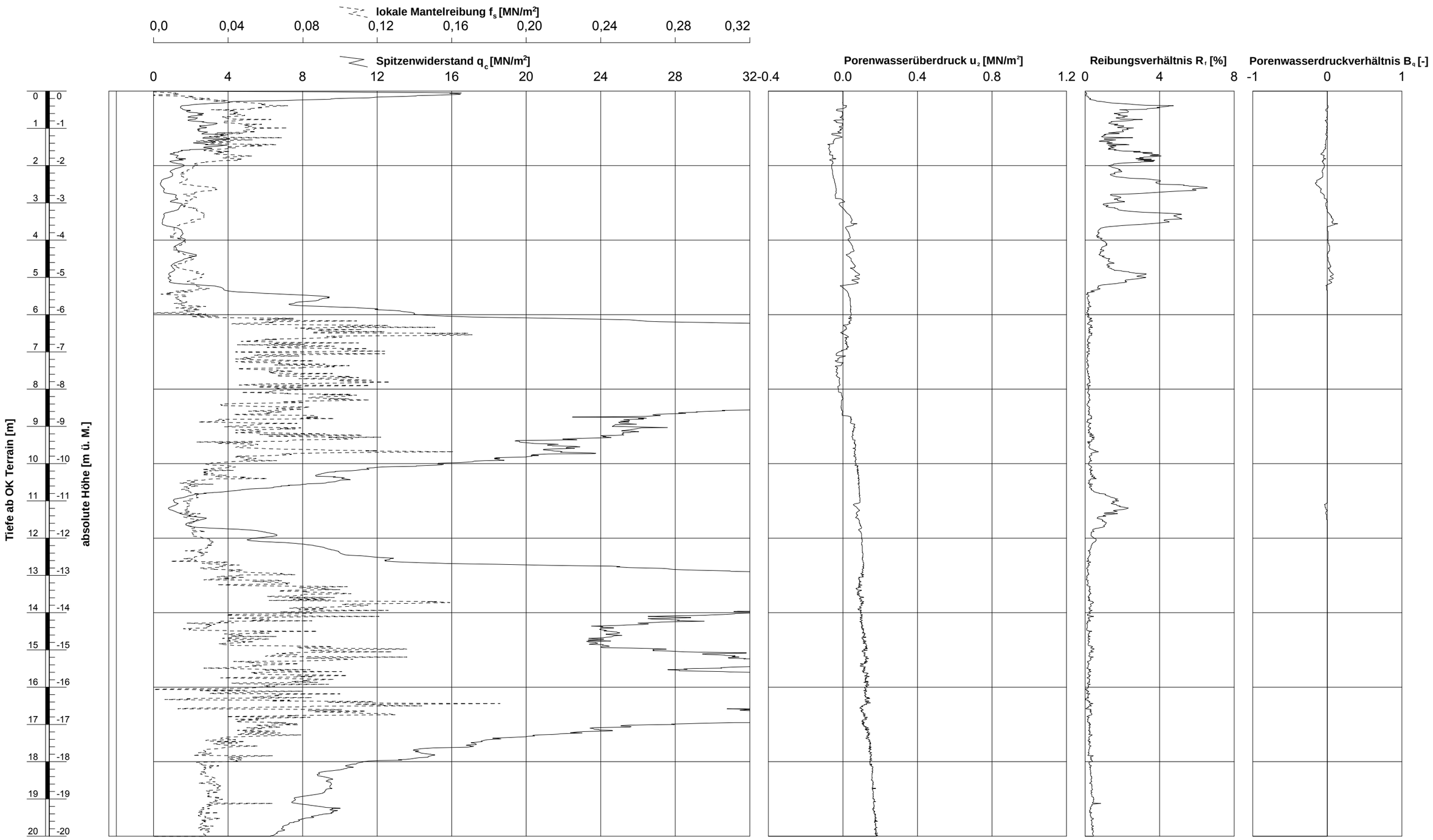

Ausführungsdatum : 21.04.2016
Ansatzpunkt : 0.00 m ü. M.
Wasser : m ab OK Terrain

Koordinaten: : 0.0 m O
0.0 m N

Messsonde : S15CFIIP15
Spitzenquerschnitt: 15 cm²

ELEKTRISCHE DRUCKSONDIERUNG
Messdaten
Hospital Rennaz

Sondierung: CPTU 1

gezeichnet: Virginia Herrera dd: kontrolliert:

GeODin-System / CPT Daten A3 CH 1_100_v7.GLO / 29.04.2016/14:04:00

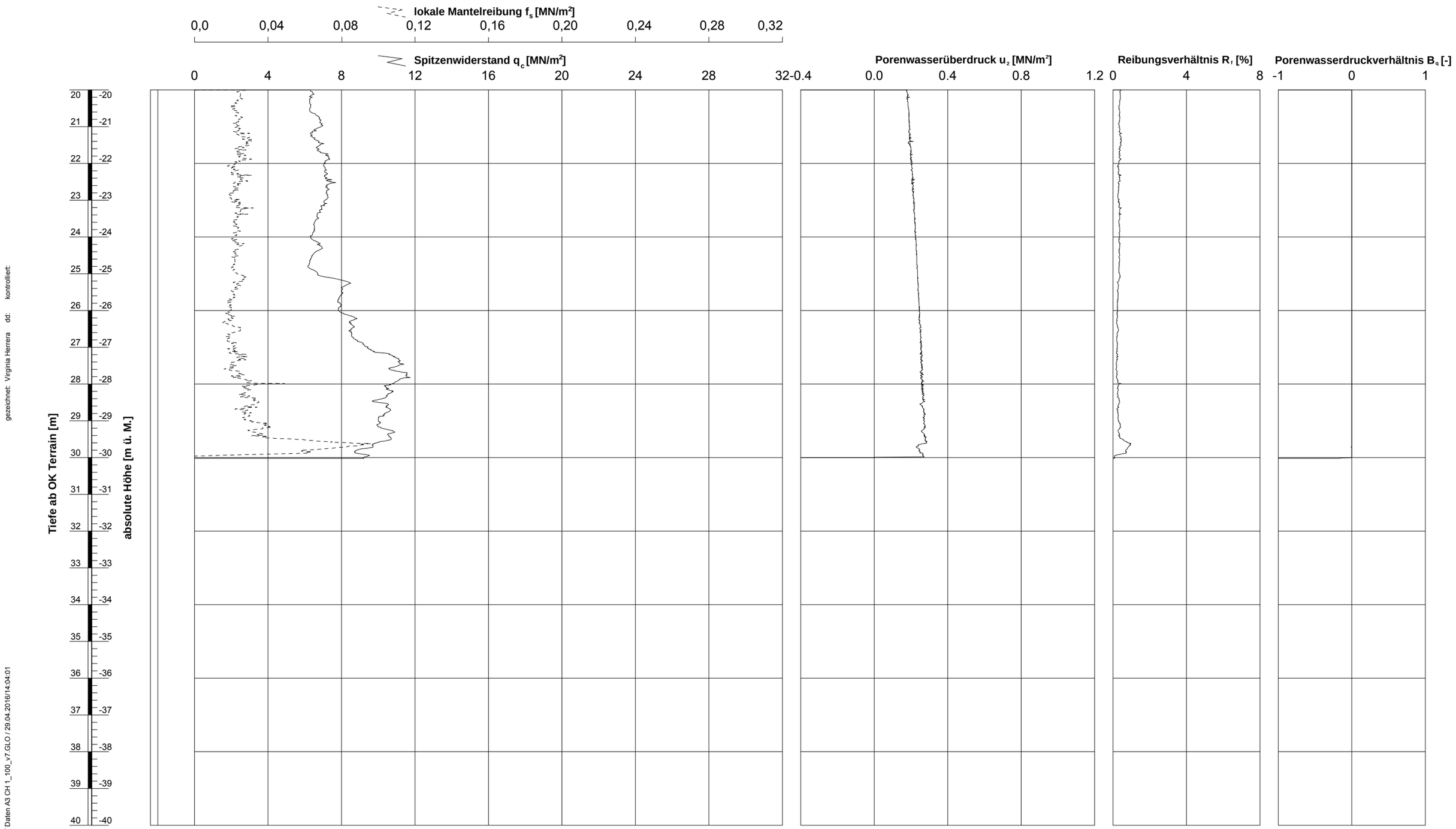

gezeichnet: Virginia Herrera dd: kontrolliert:

GeODin-System / CPT Daten A3 CH 1_100_v7.GLO / 29.04.2016/14:04:01

Ausführungsdatum : 21.04.2016
Ansatzpunkt : 0.00 m ü. M.
Wasser : m ab OK Terrain

Koordinaten: : 0.0 m O
0.0 m N

Messsonde : S15CFIIP15
Spitzenquerschnitt: 15 cm²

ELEKTRISCHE DRUCKSONDIERUNG
Messdaten
Hospital Rennaz

Sondierung: CPTU 1

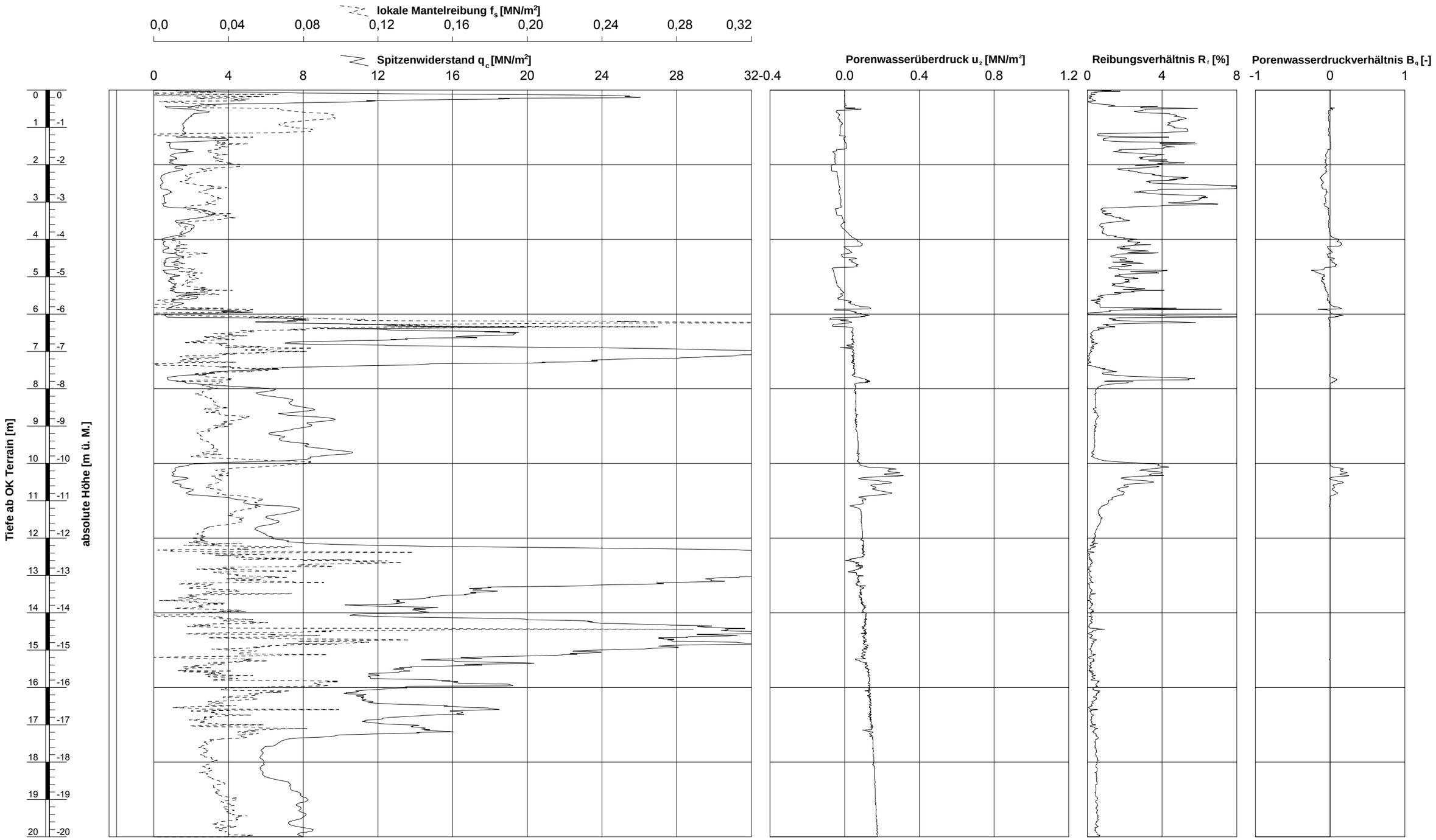

gezeichnet: Virginia Herrera dd: kontrolliert:

Ausführungsdatum : 21.04.2016
Ansatzpunkt : 0.00 m ü. M.
Wasser : m ab OK Terrain

Koordinaten: : 0.0 m O
0.0 m N

Messsonde : S15CFIIP15
Spitzenquerschnitt: 15 cm²

ELEKTRISCHE DRUCKSONDIERUNG
Messdaten
Hospital Rennaz

Sondierung: CPTU 2

GeODin-System / CPT Daten A3 CH 1_100_v7.GLO / 29.04.2016/14:21:24

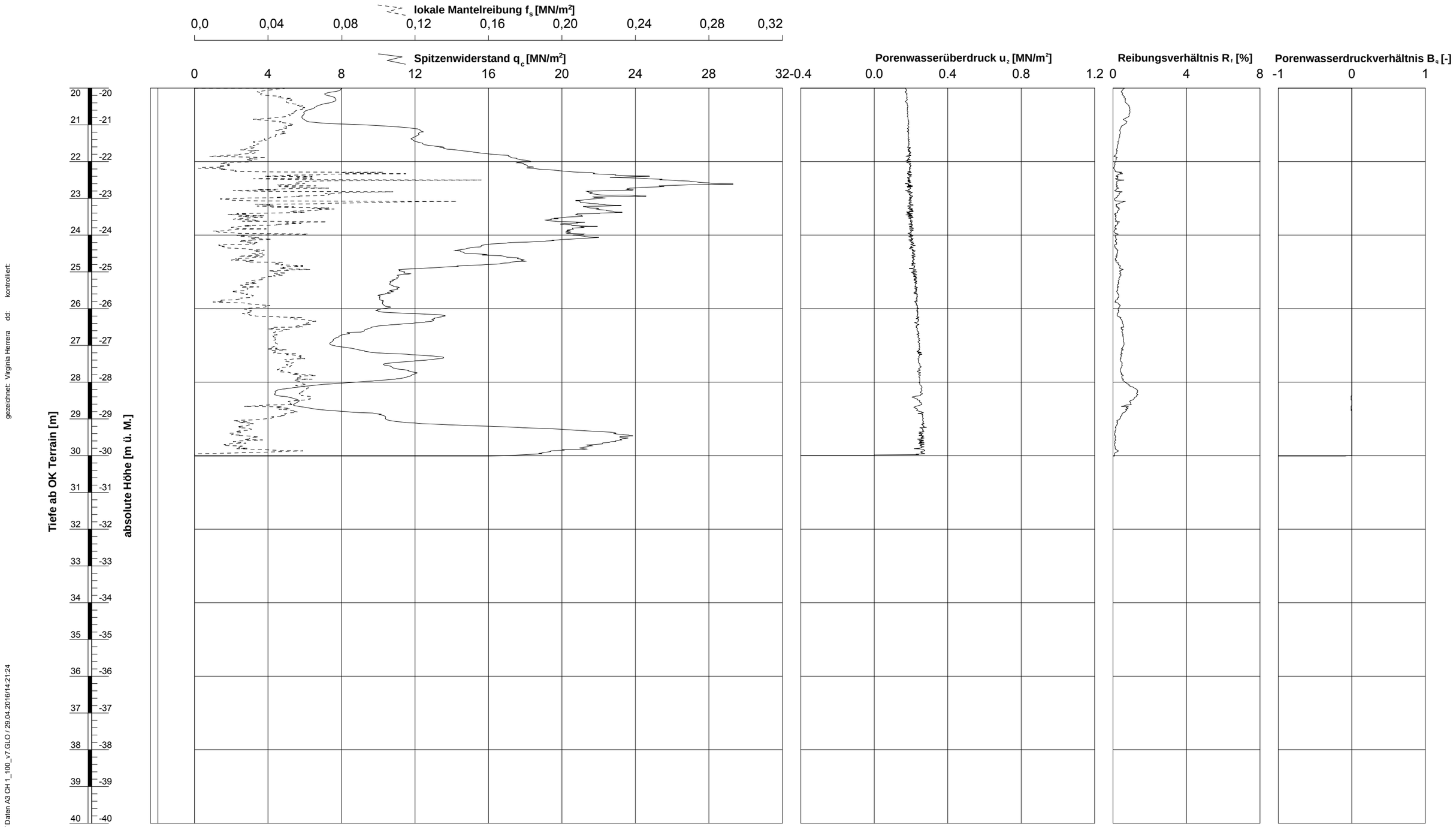

gezeichnet: Virginia Herrera dd: kontrolliert:

GeODin-System / CPT Daten A3 CH 1_100_v7.GLO / 29.04.2016/14:21:24

Ausführungsdatum : 21.04.2016
Ansatzpunkt : 0.00 m ü. M.
Wasser : m ab OK Terrain

Koordinaten: : 0.0 m O
0.0 m N

Messsonde : S15CFIIP15
Spitzenquerschnitt: 15 cm²

ELEKTRISCHE DRUCKSONDIERUNG
Messdaten
Hospital Rennaz

Sondierung: CPTU 2

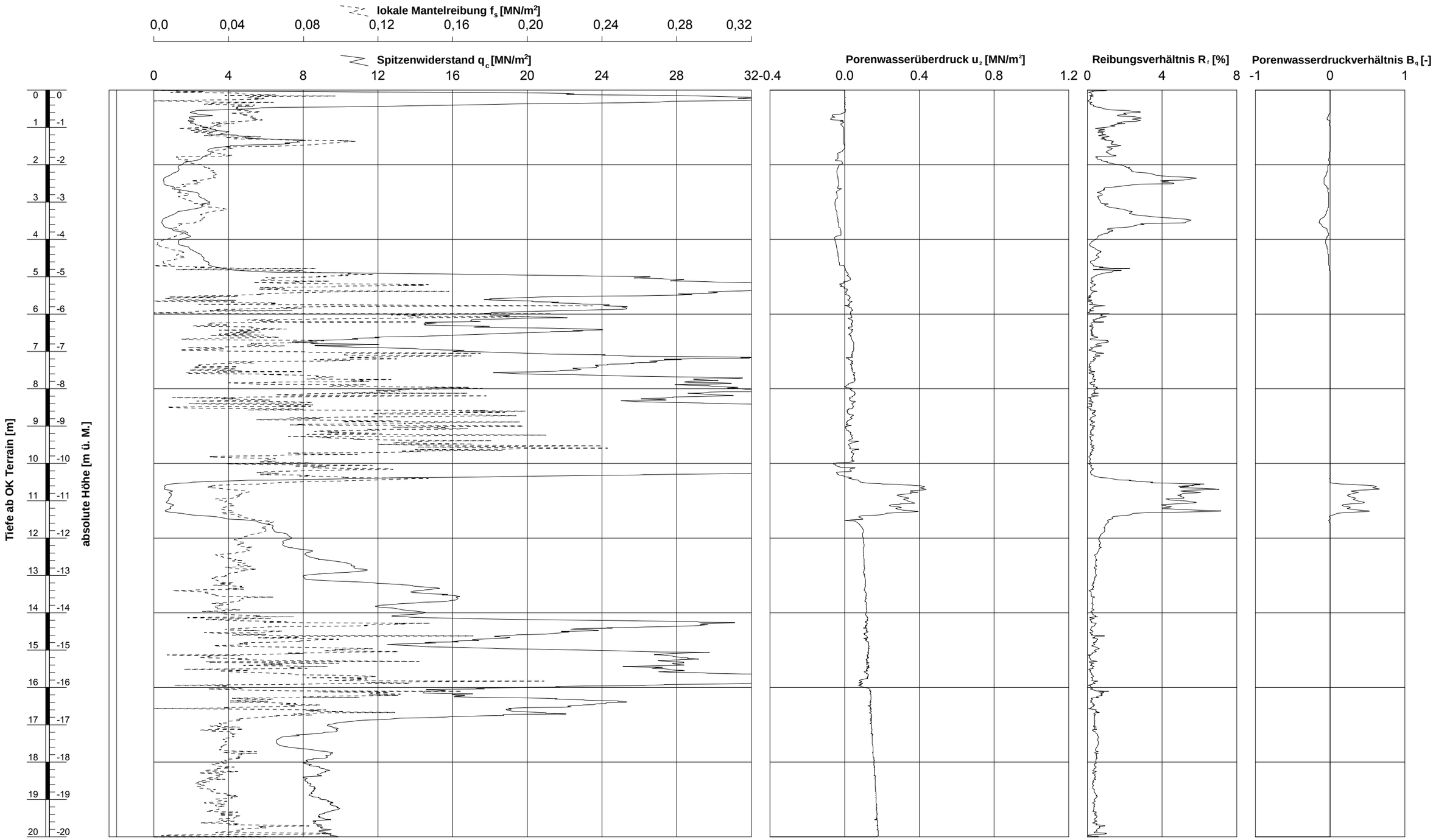

gezeichnet: Virginia Herrera dd: kontrolliert:

Ausführungsdatum : 21.04.2016
Ansatzpunkt : 0.00 m ü. M.
Wasser : m ab OK Terrain

Koordinaten: : 0.0 m O
0.0 m N

Messsonde : S15CFIIP15
Spitzenquerschnitt: 15 cm²

ELEKTRISCHE DRUCKSONDIERUNG
Messdaten
Hospital Rennaz

Sondierung: CPTU 3

GeODin-System / CPT Daten A3 CH 1_100_v7.GLO / 29.04.2016/14:24:48

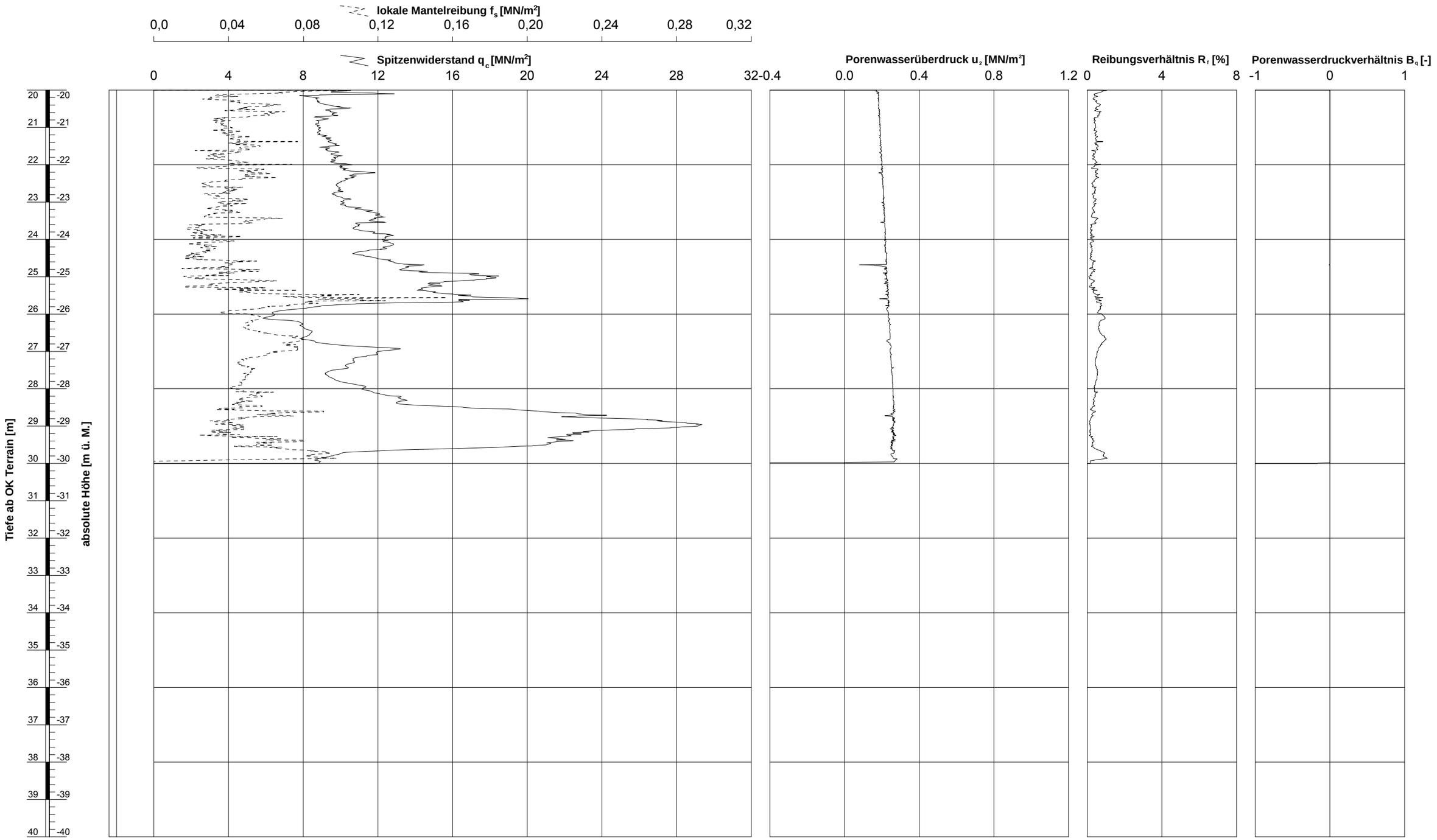

gezeichnet: Virginia Herrera dd: kontrolliert:

GeODin-System / CPT Daten A3 CH 1_100_v7.GLO / 29.04.2016/14:24:49

Ausführungsdatum : 21.04.2016
Ansatzpunkt : 0.00 m ü. M.
Wasser : m ab OK Terrain

Koordinaten: : 0.0 m O
0.0 m N

Messsonde : S15CFIIP15
Spitzenquerschnitt: 15 cm²

ELEKTRISCHE DRUCKSONDIERUNG
Messdaten
Hospital Rennaz

Sondierung: CPTU 3

BEILAGE C

ELEKTRISCHE DRUCKSONDIERUNG - INTERPRETATION

INHALT Beilage

GEOPROFILE

+ undrainierte Scherfestigkeit c_u [kN/m²]
○ Sensitivität S_t [-]

× effektiver innerer Reibungswinkel ϕ [°]
· effektive Kohäsion c' [kN/m²]

△ bezogene Lagerungsdichte I_D [-]

□ Vorkonsolidierungsdruck σ'_p [kN/m²]
+ oedometrischer Steifemodul bei Erstbelastung E_{oed} (früher: $M_{E,1}$ bzw. E_s) [MN/m²]

geotechnische Beschreibung

0.00 m: KIES, sandig, sehr dicht gelagert (künstliche Auffüllungen)

0.35 m: SAND, siltig, tonig, kiesig, locker bis mitteldicht gelagert

1.60 m: SILT, stark sandig, mittelsteif, mit Zwischenschichten aus weichem Ton und siltigem, locker gelagertem Sand

5.10 m: KIES, sehr dicht gelagert

8.70 m: KIES, sandig, mitteldicht bis dicht gelagert

10.80 m: SILT, stark tonig, mittelsteif, mit Zwischenschichten aus Sand

11.80 m: KIES, sandig, dicht gelagert

18.00 m: SAND, lagenweise feinkiesig, locker bis mitteldicht gelagert

Tiefe ab OK Terrain [m]

absolute Höhe [m ü. M.]

undrainierte Scherfestigkeit

1 10 100 1000

sehr weich | weich | mittelsteif | steif | hart | sehr hart

drainierte Scherfestigkeit

0 20 40 60

Lagerungsdichte

0.0 0.5 1.0

sehr locker | locker | mitteldicht | dicht | sehr dicht

In-situ Spannungsverhältnisse / Deformationseigenschaften

1 10 100 1000

Ausführungsdatum : 21.04.2016
Ansatzpunkt : 0.00

Koordinaten : 0.0 m O
0.0 m N

Sondierung: CPTU 1

ELEKTRISCHE DRUCKSONDIERUNG
Interpretierte geotechnische Erwartungswerte
Hospital Rennaz

gezeichnet: vhm Datum: 22.04.2016 kontrolliert: cfa

GeODin-System / CPT Interp A3 CH 1_100_v7 GLO / 02.05.2016/12:26:22

+ undrainierte Scherfestigkeit c_u [kN/m²]
○ Sensitivität S_t [-]

× effektiver innerer Reibungswinkel ϕ [°]
· effektive Kohäsion c' [kN/m²]

△ bezogene Lagerungsdichte I_D [-]

□ Vorkonsolidierungsdruck σ'_p [kN/m²]
+ oedometrischer Steifemodul bei Erstbelastung E_{oed} (früher: $M_{E,1}$ bzw. E_s) [MN/m²]

geotechnische Beschreibung

18.00 m: SAND, lagenweise feinkiesig, locker bis mitteldicht gelagert

25.10 m: SAND, feinkiesig, mitteldicht gelagert

undrainierte Scherfestigkeit

1 10 100 1000

sehr weich | weich | mittel steif | steif | hart | sehr hart

drainierte Scherfestigkeit

0 20 40 60

Lagerungsdichte

0.0 0.5 1.0

sehr locker | locker | mittel dicht | dicht | sehr dicht

In-situ Spannungsverhältnisse / Deformationseigenschaften

1 10 100 1000

Tiefe ab OK Terrain [m] 20 21 22 23 24 25 26 27 28 29 30 31 32 33 34 35 36 37 38 39 40

absolute Höhe [m ü. M.] -20 -21 -22 -23 -24 -25 -26 -27 -28 -29 -30 -31 -32 -33 -34 -35 -36 -37 -38 -39 -40

Ausführungsdatum : 21.04.2016
Ansatzpunkt : 0.00

Koordinaten : 0.0 m O
0.0 m N

Sondierung: CPTU 1

ELEKTRISCHE DRUCKSONDIERUNG
Interpretierte geotechnische Erwartungswerte
Hospital Rennaz

gezeichnet: vhm Datum: 22.04.2016 kontrolliert: cfa

GeODin-System / CPT Interp A3 CH 1_100_v7.GLO / 02.05.2016/12:26:23

+ undrainierte Scherfestigkeit c_u[kN/m²]
○ Sensitivität S_t [-]
× effektiver innerer Reibungswinkel ϕ [°]
· effektive Kohäsion c' [kN/m²]
△ bezogene Lagerungsdichte I_D[-]
□ Vorkonsolidierungsdruck σ'_p [kN/m²]
+ oedometrischer Steifemodul bei Erstbelastung E_{oed} (früher: $M_{E,1}$ bzw. E_s) [MN/m²]

geotechnische Beschreibung

0.00 m: KIES, sehr dicht gelagert (künstliche Auffüllungen)

0.45 m: TON, lagenweise stark siltig, lokal kiesig, weich bis mittelsteif, mit Zwischenschichten aus locker gelagertem Sand

6.30 m: KIES, mitteldicht bis dicht gelagert

7.60 m: SAND, mitteldicht gelagert, mit Zwischenschichten aus mittelsteifem Ton und siltigem Ton

12.10 m: KIES, sandig bis stark sandig, mitteldicht bis dicht gelagert

17.40 m: SAND, locker bis mitteldicht gelagert

Tiefe ab OK Terrain [m]

absolute Höhe [m ü. M.]

undrainierte Scherfestigkeit

1 10 100 1000

sehr weich | weich | mittel steif | steif | hart | sehr hart

drainierte Scherfestigkeit

0 20 40 60

Lagerungsdichte

0.0 0.5 1.0

sehr locker | locker | mittel dicht | dicht | sehr dicht

In-situ Spannungsverhältnisse / Deformationseigenschaften

1 10 100 1000

Ausführungsdatum : 21.04.2016
Ansatzpunkt : 0.00

Koordinaten : 0.0 m O
0.0 m N

ELEKTRISCHE DRUCKSONDIERUNG
Interpretierte geotechnische Erwartungswerte
Hospital Rennaz

Sondierung: CPTU 2

gezeichnet: vhm Datum: 22.04.2016 kontrolliert: cfa

GeODin-System / CPT Interp A3 CH 1_100_v7.GLO / 02.05.2016/12:15:38

+ undrainierte Scherfestigkeit c_u[kN/m²]
○ Sensitivität S_t [-]
× effektiver innerer Reibungswinkel ϕ [°]
· effektive Kohäsion c' [kN/m²]
△ bezogene Lagerungsdichte I_D[-]
□ Vorkonsolidierungsdruck σ'_p [kN/m²]
+ oedometrischer Steifemodul bei Erstbelastung E_{oed} (früher: $M_{E,1}$ bzw. E_s) [MN/m²]

gezeichnet: vhm Datum: 22.04.2016 kontrolliert: cfa

geotechnische Beschreibung

17.40 m: SAND, locker bis mitteldicht gelagert

21.00 m: SAND, kiesig, mitteldicht gelagert

24.80 m: SAND, lagenweise feinkiesig, mitteldicht gelagert

28.00 m: SAND, locker gelagert

28.70 m: SAND, feinkiesig, mitteldicht gelagert

undrainierte Scherfestigkeit

1 10 100 1000

sehr weich | weich | mittel steif | steif | hart | sehr hart

drainierte Scherfestigkeit

0 20 40 60

Lagerungsdichte

0.0 0.5 1.0

sehr locker | locker | mittel dicht | dicht | sehr dicht

In-situ Spannungsverhältnisse / Deformationseigenschaften

1 10 100 1000

Tiefe ab OK Terrain [m] 20 21 22 23 24 25 26 27 28 29 30 31 32 33 34 35 36 37 38 39 40

absolute Höhe [m ü. M.] -20 -21 -22 -23 -24 -25 -26 -27 -28 -29 -30 -31 -32 -33 -34 -35 -36 -37 -38 -39 -40

Ausführungsdatum : 21.04.2016
Ansatzpunkt : 0.00

Koordinaten : 0.0 m O
0.0 m N

Sondierung: CPTU 2

ELEKTRISCHE DRUCKSONDIERUNG
Interpretierte geotechnische Erwartungswerte
Hospital Rennaz

GeODin-System / CPT Interp A3 CH 1_100_v7.GLO / 02.05.2016/12:15:39

GEOPROFILE

+ undrainierte Scherfestigkeit c_u[kN/m²]
○ Sensitivität S_t [-]

× effektiver innerer Reibungswinkel ϕ [°]
· effektive Kohäsion c' [kN/m²]

△ bezogene Lagerungsdichte I_D[-]

□ Vorkonsolidierungsdruck σ'_p [kN/m²]
+ oedometrischer Steifemodul bei Erstbelastung E_{oed} (früher: $M_{E,1}$ bzw. E_s) [MN/m²]

gezeichnet: vhm Datum: 22.04.2016 kontrolliert: cfa

geotechnische Beschreibung

0.00 m: KIES, sehr dicht gelagert (künstliche Auffüllungen)
0.50 m: SAND, siltig, locker gelagert, mit Zwischenschichten aus Silt und Ton
4.70 m: KIES, dicht bis sehr dicht gelagert, mit Zwischenschichten aus mitteldicht gelagertem Sand
10.50 m: TON, weich bis mittelsteif
11.50 m: SAND, kiesig, mitteldicht gelagert
14.10 m: KIES, sandig, mitteldicht bis dicht gelagert
16.90 m: SAND, kiesig, mitteldicht gelagert

Tiefe ab OK Terrain [m]
absolute Höhe [m ü. M.]

undrainierte Scherfestigkeit

1 10 100 1000
sehr weich | weich | mittel steif | steif | hart | sehr hart

drainierte Scherfestigkeit

0 20 40 60

Lagerungsdichte

0.0 0.5 1.0
sehr locker | locker | mittel dicht | dicht | sehr dicht

In-situ Spannungsverhältnisse / Deformationseigenschaften

1 10 100 1000

Ausführungsdatum : 21.04.2016
Ansatzpunkt : 0.00
Koordinaten : 0.0 m O
0.0 m N

Sondierung: CPTU 3

ELEKTRISCHE DRUCKSONDIERUNG
Interpretierte geotechnische Erwartungswerte
Hospital Rennaz

GeODin-System / CPT Interp A3 CH 1_100_v7.GLO / 02.05.2016/12:26:03

+ undrainierte Scherfestigkeit c_u[kN/m²]
○ Sensitivität S_t [-]

× effektiver innerer Reibungswinkel ϕ [°]
· effektive Kohäsion c' [kN/m²]

△ bezogene Lagerungsdichte I_D[-]

□ Vorkonsolidierungsdruck σ'_p [kN/m²]
+ oedometrischer Steifemodul bei Erstbelastung E_{oed} (früher: $M_{E,1}$ bzw. E_s) [MN/m²]

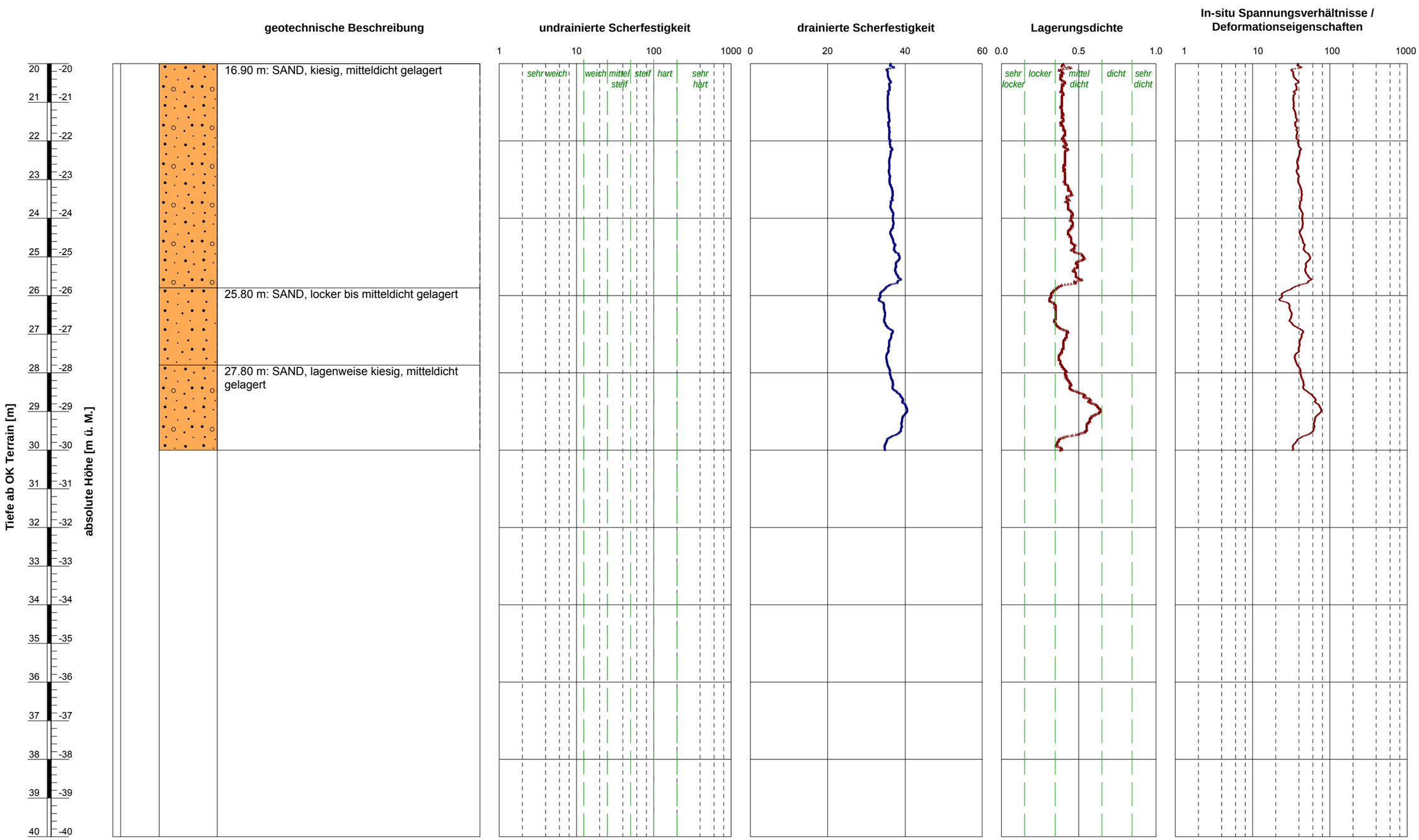

Ausführungsdatum : 21.04.2016
Ansatzpunkt : 0.00

Koordinaten : 0.0 m O
0.0 m N

Sondierung: CPTU 3

ELEKTRISCHE DRUCKSONDIERUNG
Interpretierte geotechnische Erwartungswerte
Hospital Rennaz

gezeichnet: vhm Datum: 22.04.2016 kontrolliert: cfa

GeODin-System / CPT Interp A3 CH 1_100_v7.GLO / 02.05.2016/12:26:03

BEILAGE D

ANALYSE DES BODENVERFLÜSSIGUNGSPOTENZIALS

INHALT Beilage

BEMERKUNGEN ZUR ANALYSE

Analysemethode

Die Bestimmung des Bodenverflüssigungspotenzials, welches sich primär auf sandigen Schichten bezieht, richtet sich nach dem Verfahren gemäss Robertson und Wride (1998) und Robertson (2009):

1. Bestimmung des Schichtaufbaus des Untergrundes aufgrund von elektrischen Drucksondierungen;
2. Bestimmung der zyklischen Erdbebenlast aufgrund der zu erwartenden, maximalen horizontalen Bodenbeschleunigung (cyclic stress ratio, CSR);
3. Bestimmung des Widerstands der einzelnen Schichten gegen einer zyklischen Erdbebenlast für Sandschichten (cyclic resistance ratio, CRR);
4. Bestimmung der Wahrscheinlichkeit einer Verflüssigung von Sanden aufgrund historischer Daten.

Anhang 3 dokumentiert die oben erwähnten Analysemethoden im Detail.

Gemäss der Seismischen Mikrozonierung des Rhônetals im Kanton Waadt[1)] liegt Rennaz in Zone S5. Gemäss der Erdbebengefährdungskarte des Schweizerischen Erdbebendienstes liegt Rennaz in Gefährdungszone Z3a, womit als Bemessungswert für die horizontale Bodenbeschleunigung a_{gd} 1.3 m/s^2 anzunehmen ist. Zudem wurde angenommen, dass der Grundwasserspiegel im Falle eines Erdbebens 1 m unter OK Terrain liegt. Es handelt sich bei dem geplanten Neubau um ein Bauwerk der Klasse III.
Der Analyse wurden Beben der Magnituden 5.5, 6.0 und 6.5 zugrunde gelegt.

Die Analyse von Sondierungen lässt für alle untersuchten Magnituden über grosse Abschnitte des Profils Bodenverflüssigungspotential erkennen.

[1)] Microzonage sismique spectral de la vallée du Rhône vaudois 2009

Geoprofile GmbH
Ebikonerstrasse 42
6043 Adligenswil
www.geoprofile.ch

LIQUEFACTION ANALYSIS REPORT

Project title : 60-748 Hopital Rennaz **Location :**

CPT file : Interp CPTU 2

Input parameters and analysis data

Analysis method:	Robertson (2009)	G.W.T. (in-situ):	1.00 m	Use fill:	No	Clay like behavior applied:	All soils
Fines correction method:	Robertson (2009)	G.W.T. (earthq.):	1.00 m	Fill height:	N/A	Limit depth applied:	No
Points to test:	Based on Ic value	Average results interval:	3	Fill weight:	N/A	Limit depth:	N/A
Earthquake magnitude M_w:	5.50	Ic cut-off value:	2.60	Trans. detect. applied:	Yes		
Peak ground acceleration:	0.22	Unit weight calculation:	Based on SBT	K_σ applied:	No		

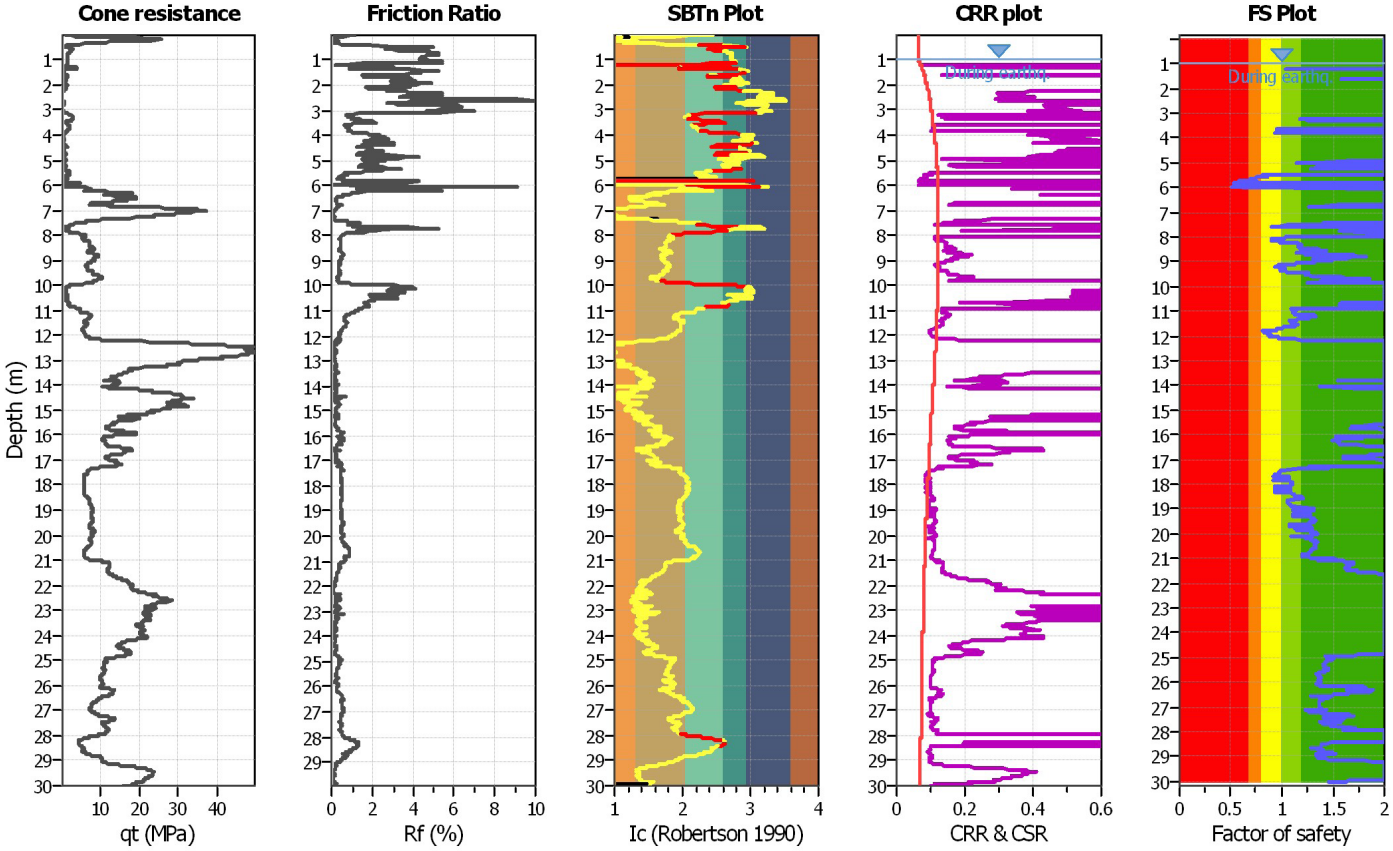

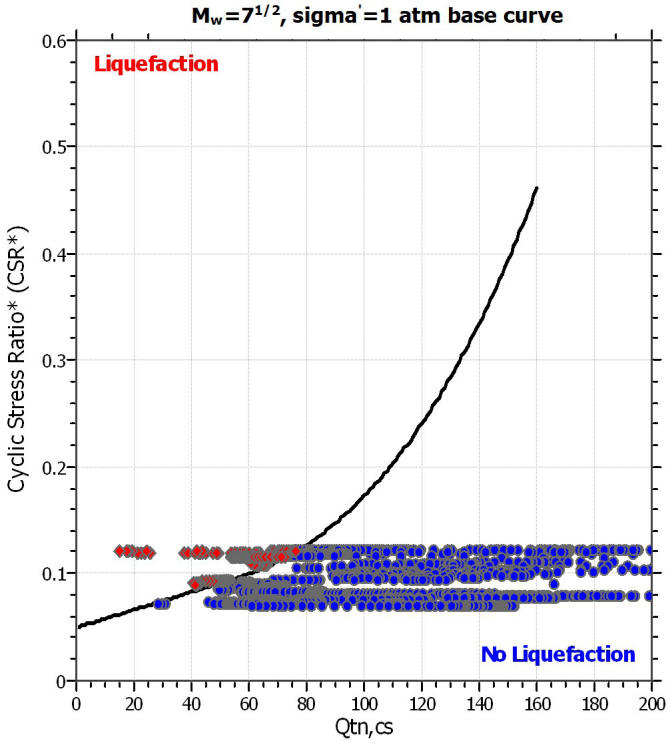

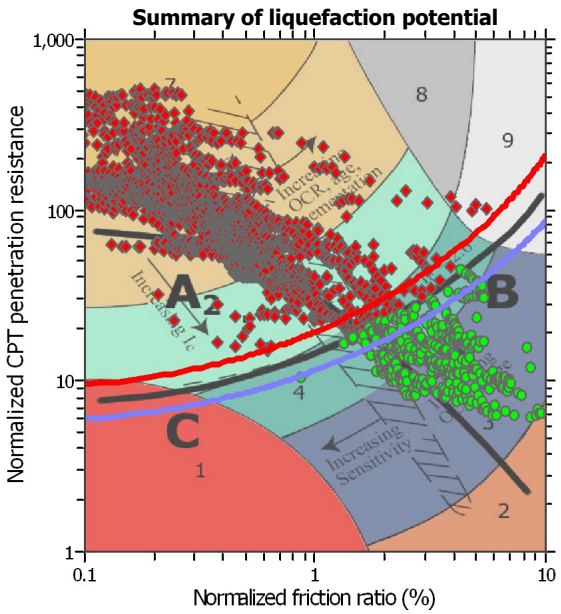

Zone A_1: Cyclic liquefaction likely depending on size and duration of cyclic loading
Zone A_2: Cyclic liquefaction and strength loss likely depending on loading and ground geometry
Zone B: Liquefaction and post-earthquake strength loss unlikely, check cyclic softening
Zone C: Cyclic liquefaction and strength loss possible depending on soil plasticity, brittleness/sensitivity, strain to peak undrained strength and ground geometry

Geoprofile GmbH
Ebikonerstrasse 42
6043 Adligenswil
www.geoprofile.ch

LIQUEFACTION ANALYSIS REPORT

Project title : 60-748 Hopital Rennaz **Location :**

CPT file : Interp CPTU 2

Input parameters and analysis data

Analysis method:	Robertson (2009)	G.W.T. (in-situ):	1.00 m	Use fill:	No	Clay like behavior applied:	All soils
Fines correction method:	Robertson (2009)	G.W.T. (earthq.):	1.00 m	Fill height:	N/A	Limit depth applied:	No
Points to test:	Based on Ic value	Average results interval:	3	Fill weight:	N/A	Limit depth:	N/A
Earthquake magnitude M_w:	6.00	Ic cut-off value:	2.60	Trans. detect. applied:	Yes		
Peak ground acceleration:	0.22	Unit weight calculation:	Based on SBT	K_σ applied:	No		

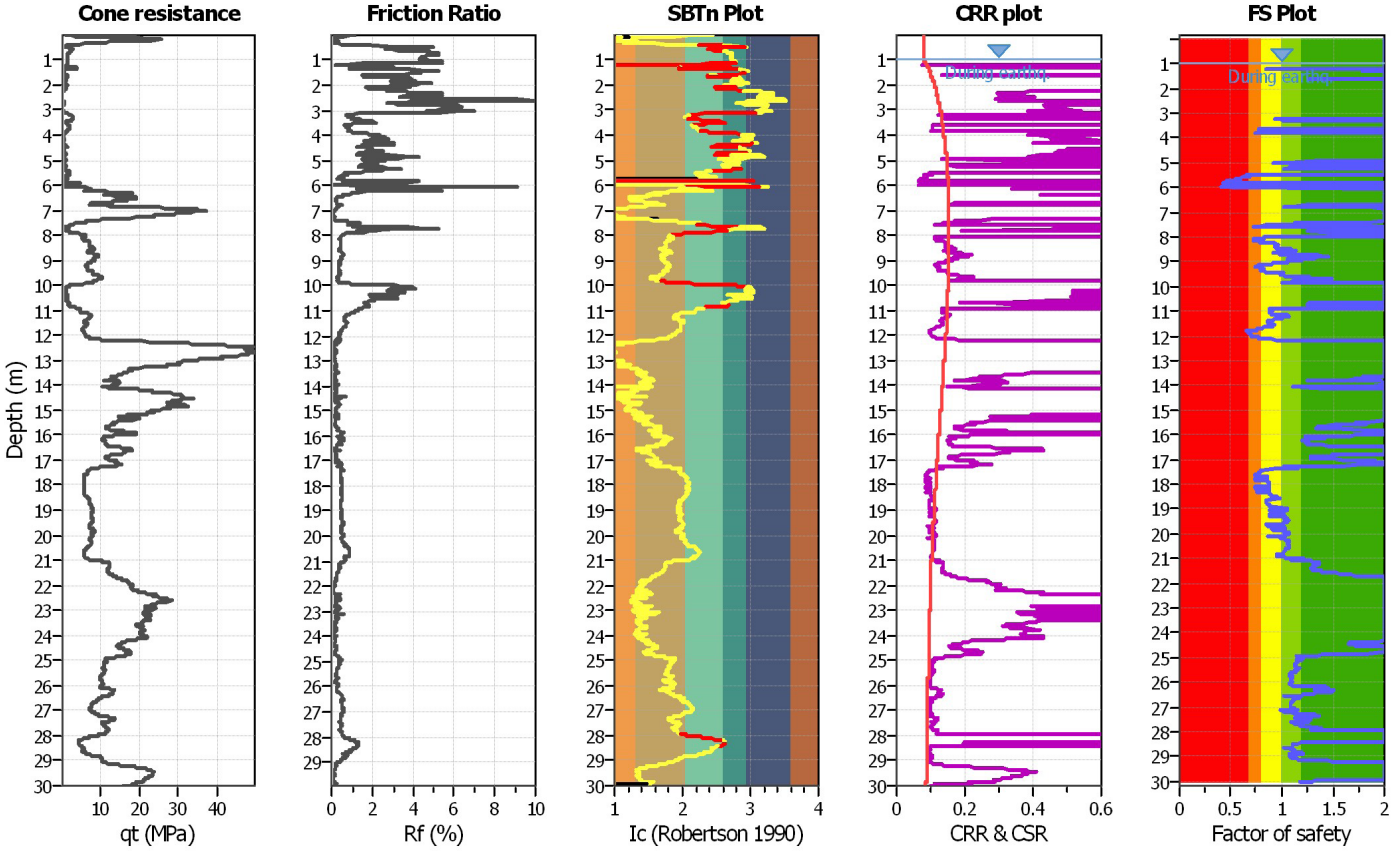

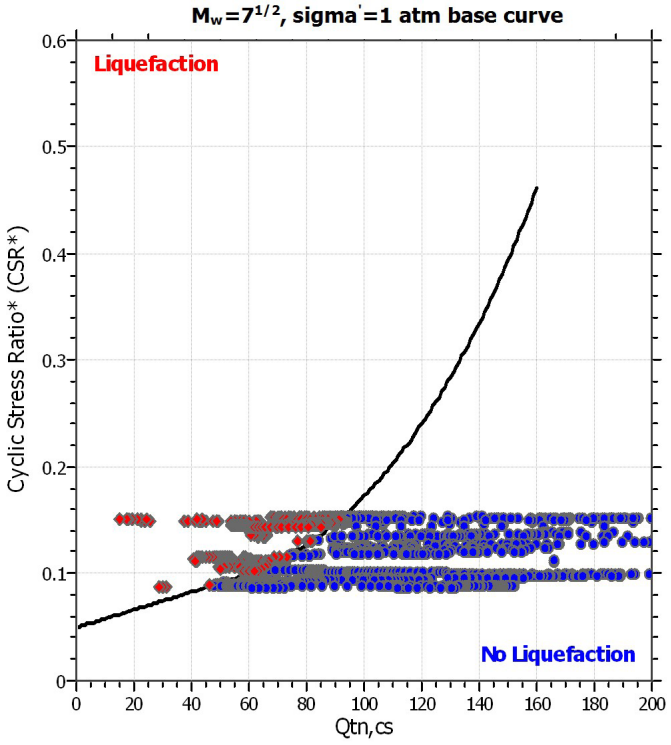

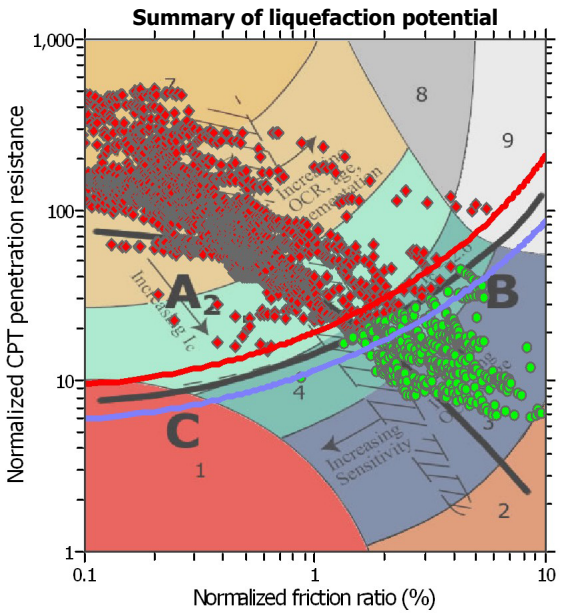

Zone A_1: Cyclic liquefaction likely depending on size and duration of cyclic loading
Zone A_2: Cyclic liquefaction and strength loss likely depending on loading and ground geometry
Zone B: Liquefaction and post-earthquake strength loss unlikely, check cyclic softening
Zone C: Cyclic liquefaction and strength loss possible depending on soil plasticity, brittleness/sensitivity, strain to peak undrained strength and ground geometry

Geoprofile GmbH
Ebikonerstrasse 42
6043 Adligenswil
www.geoprofile.ch

LIQUEFACTION ANALYSIS REPORT

Project title : 60-748 Hopital Rennaz **Location :**

CPT file : Interp CPTU 2

Input parameters and analysis data

Analysis method:	Robertson (2009)	G.W.T. (in-situ):	1.00 m	Use fill:	No	Clay like behavior applied:	All soils
Fines correction method:	Robertson (2009)	G.W.T. (earthq.):	1.00 m	Fill height:	N/A	Limit depth applied:	No
Points to test:	Based on Ic value	Average results interval:	3	Fill weight:	N/A	Limit depth:	N/A
Earthquake magnitude M_w:	6.50	Ic cut-off value:	2.60	Trans. detect. applied:	Yes		
Peak ground acceleration:	0.22	Unit weight calculation:	Based on SBT	K_σ applied:	No		

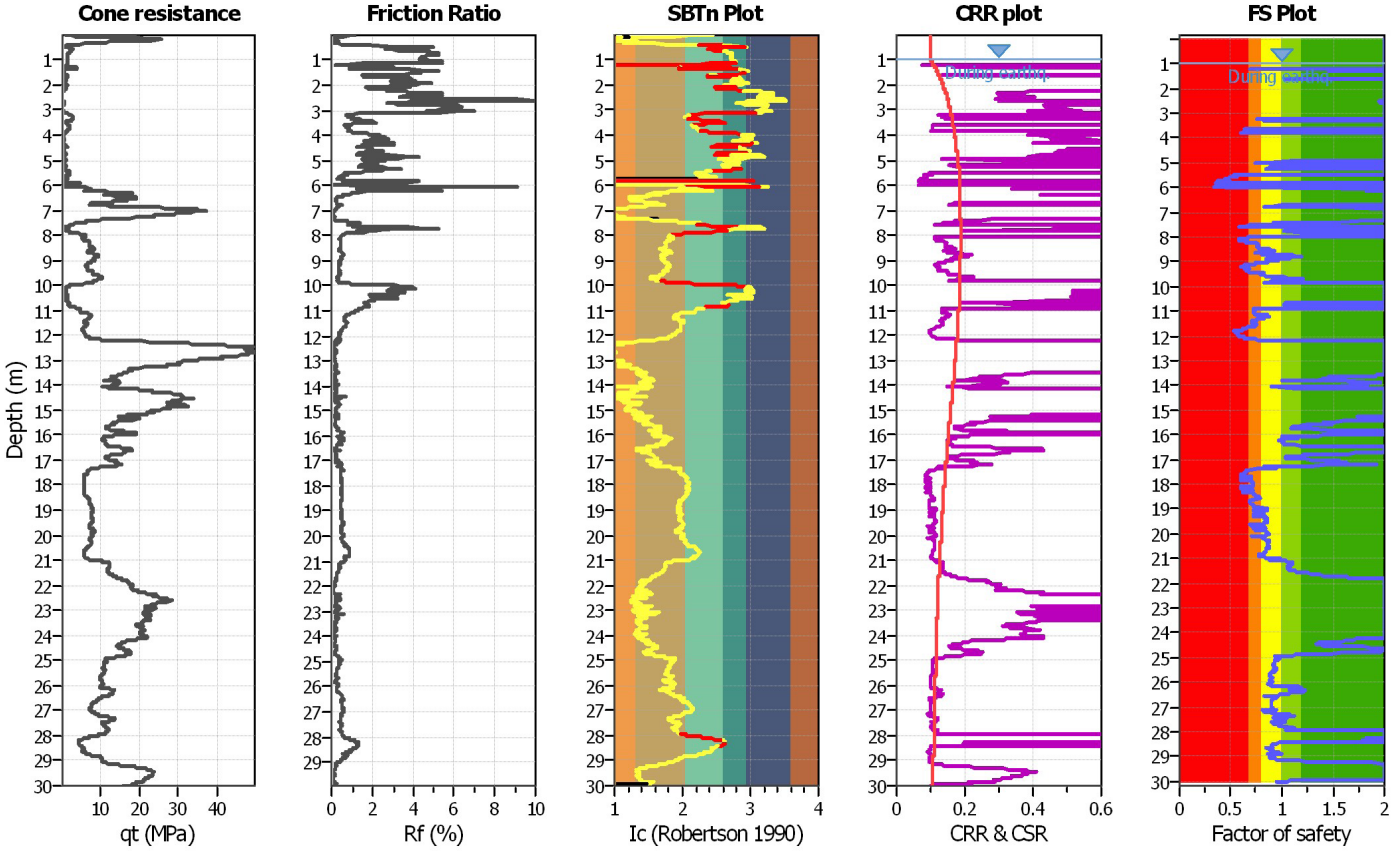

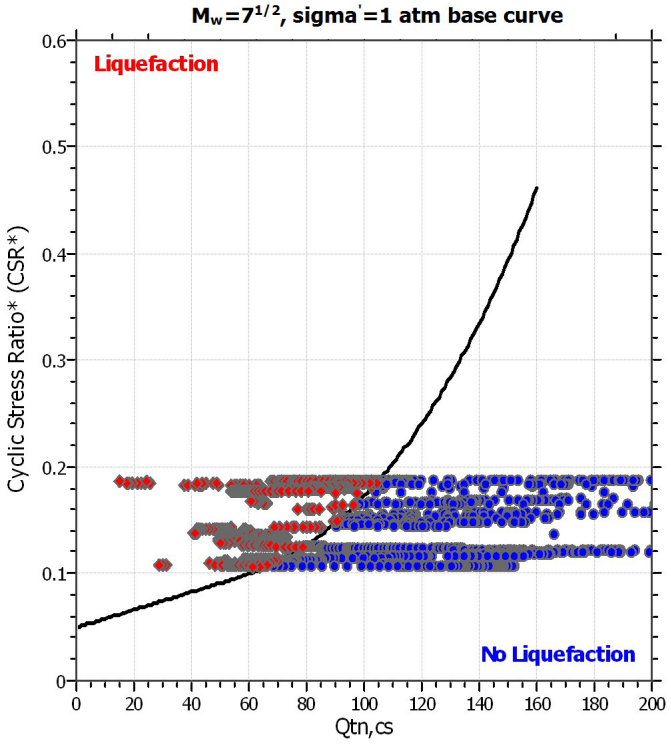

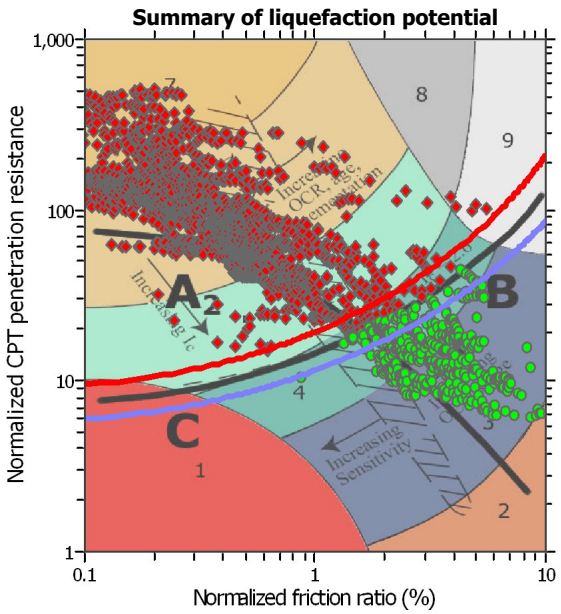

Zone A_1: Cyclic liquefaction likely depending on size and duration of cyclic loading
Zone A_2: Cyclic liquefaction and strength loss likely depending on loading and ground geometry
Zone B: Liquefaction and post-earthquake strength loss unlikely, check cyclic softening
Zone C: Cyclic liquefaction and strength loss possible depending on soil plasticity, brittleness/sensitivity, strain to peak undrained strength and ground geometry

ANHÄNGE

ALLGEMEINE HINTERGRUNDINFORMATION

INHALT

ALLGEMEINES

Die Drucksondierung (CPT) ist ein Verfahren, das häufig zur Untersuchung des Baugrunds verwendet wird. Hierbei wird der Widerstand des Baugrunds bei konstantem und kontinuierlichem Eindringen mit einem zylindrischen und mit internen Sensoren ausgestatteten Penetrometer bestimmt. Gemessen werden Eindringtiefe (z), Spitzenwiderstand (q_c), lokale Mantelreibung (f_s) und ggf. Porenwasserdruck (u_2) und der vertikale Neigungswinkel (i_x bzw. i_y). Die Ergebnisse ermöglichen eindeutige Rückschlüsse auf die Beschaffenheit des Baugrunds.

Die von Geoprofile für die Drucksondierung angewandten Verfahren und verwendeten Geräte richten sich nach ISO EN 22476-1 und den Regelungen der Veröffentlichung “International Reference Test Procedure” der internationalen Gesellschaft für Grundbau und Bodenmechanik (ISSMGE, 1999).

Wenn nicht anders vereinbart, gelten die folgenden Kriterien für die Beendigung des Versuchs:
- das Erreichen der gewünschten Eindringtiefe,
- die Abweichung von der Vertikale ist grösser als 15^o,
- die Abweichung von der Vertikale vergrössert sich plötzlich,
- das Erreichen der Höchstleistung des Druckgerätes, der Auflagevorrichtung, der Schubstangen und/oder der Messsensoren,
- Umstände im Ermessen des Sondiermeisters, wie z.B. das Risiko von Sach- oder Personenschaden.

ERGEBNISSE

Die Darstellung der Ergebnisse der Drucksondierungen umfasst:
- die Parameter q_c, f_s und R_f sowie u_2 in Abhängigkeit der Tiefe unter der Erdoberfläche,
- fakultativ die Parameter q_t, q_n und B_q bei Versuchen mit Porendruckmessungen,
- fakultativ den Neigungswinkel i bei Versuchen mit Winkelmessungen.

Als Bezugswert der Versuche gilt die Erdoberfläche. Die Definition der einzelnen Parameter ist wie folgt:

z = Eindringtiefe in die Erdoberfläche, bezüglich des vertikalen Neigungswinkels (i) korrigiert:

$$= \int_0^l \cos i \, . \, dl$$

dabei ist:

z = Eindringtiefe

l = Eindringlänge

i = vertikaler Neigungswinkel

q_c = Spitzenwiderstand bezüglich der Referenzwerte des Versuchs.

f_s = lokale Mantelreibung. Die Tiefe wird so korrigiert, dass die (hinter der Spitze gemessene) Mantelreibung sich auf die Tiefe der Sondierspitze bezieht.

R_f = Verhältnis der Mantelreibung zum Spitzenwiderstand (f_s/q_c).

u_2 = Porendruck direkt hinter der Sondierspitze (Position 2). Die Tiefe wird so korrigiert, dass der gemessene Porenwasserdruck sich auf die Tiefe der Sondierspitze bezieht.

Während der Versuchsdurchführung kann es u.U. zu einem Sättigungsverlust des Filterelementes kommen (Lunne et al., 1997). Zu den möglichen Gründen zählen:

- Eindringen in einen teilweise gesättigten Boden;
- Das Auftreten von negativem Porenwasserdruck, so dass es zu Kavitation kommt. Dies kann zum Beispiel beim Eindringen in einen dicht gelagerten Sand oder einen überkonsolidierten Ton.

Ein Sättigungsverlust führt normalerweise zu einem geringeren Porendruck beim Eindringen in den Boden unterhalb dieser Zone.

q_t = Totaler Spitzenwiderstand. Diese Kenngrösse beinhaltet Korrekturen für den hydrostatischen und den transienten Porendruck sowie für die Konstruktion der Sondierspitze:

$$q_t = q_c+(1-a)u_2$$

Dabei gilt:

a = Netto-Flächenverhältnis des Querschnitts der Stahlfläche in der Öffnung zwischen der Sondierspitze und der Reibungshülse. Dieses Verhältnis ist von der Art des Penetrometers abhängig.

q_n = $q_t-\sigma_{vo}$ = Netto-Spitzenwiderstand. Diese Kenngrösse beinhaltet Korrekturen für den hydrostatischen und den transienten Porendruck sowie für die Konstruktion der Sondierspitze und die In-Situ Spannung im Untergrund. Dabei gilt:

σ_{vo} = totale vertikale In-Situ Spannung im Bereich der Sondierspitze. Dieser Wert ist berechnet.

B_q = Porendruckverhältnis:

$B_q = (u_2-u_o)/q_n$ mit

u_o = hydrostatischer Porenwasserdruck im Bereich der Sondierspitze. Es handelt sich um einen

berechneten Wert.

WEITERE MESSUNGEN

Mit der elektrischen Drucksondierung können weitere Messungen vorgenommen werden:

- Messung des hydrostatischen Wasserdrucks in einer bestimmten Tiefe;
- Dissipations-Test. Hierbei wird die Verringerung des transienten Porenwasserdrucks als Funktion der Zeit gemessen. Die Resultate erlauben Rückschlüsse auf die horizontale Durchlässigkeit von feinkörnigen Schichten und somit auf die benötigte Zeit bis zum Abklingen der primären Setzungen.
- Prüfung des Reibungs-Aufbaus. Hierbei wird die Zunahme der lokalen Mantelreibung nach einer Unterbrechung des Sondiervorgangs gemessen. Die Resultate erlauben Rückschlüsse auf die zeitlichen Entwicklung der Mantelreibung entlang eines Pfahlschafts.

Für die Durchführung dieser zusätzlichen Messungen muss der Sondiervorgang angehalten werden.

LITERATURANGABEN

CEN (2005), “Geotechnische Erkundung und Untersuchung - Felduntersuchungen - Teil 1: Drucksondierungen mit elektrischen Messwertaufnehmern und Messeinrichtungen für den Porenwasserdruck (ISO EN 22476-1:2005)

ISSMGE International Society of Soil Mechanics and Geotechnical Engineering (1999), “International Reference Test Procedure for the Cone Penetration Test (CPT) and the Cone Penetration Test with Pore Pressure (CPTU)”, Bericht vom ISSMGE Technical Committee 16 bzgl. der Bestimmung von Baugrundeigenschaften mittels in-situ Prüfverfahren, Proceedings of the Twelfth European Conference on Soil Mechanics and Geotechnical Engineering, Amsterdam, editiert Barends et al., Vol. 3, pp. 2195-2222.

Lunne, T. (1999), “Special Workshop – Investigation Methods”, Proceedings of the Twelfth European Conference on Soil Mechanics and Geotechnical Engineering, Amsterdam, editiert Barends et al., Additional Volume, pp. 51-52.

EINLEITUNG

Das vorliegende Dokument gibt einen Überblick der verwendeten Auswertungsmethoden für die Testergebnisse von Drucksondierungen. Die Eignung der einzelnen Methoden hängt unter anderem von den Anforderungen des jeweiligen Projektes ab und muss durch einen Geotechnik-Ingenieur beurteilt werden.

Die Auswertung von Drucksondierungsversuchsergebnissen hilft bei der Festlegung von Parametern für geotechnische Modelle. Die konventionellen Modelle stützen sich normalerweise auf die Plastizitätstheorie für den Grenzzustand der Tragfähigkeit und auf die Elastizitäts- und Konsolidierungstheorie für den Grenzzustand der Gebrauchstauglichkeit (CEN, 1994). Merkmale für solche geotechnischen Modelle sind:

- eine Analyse des Verhaltens in drainiertem oder undrainiertem Zustand für Plastizitätsmodelle
- die Analyse für den Grenzzustand der Tragfähigkeit unterscheidet sich von der für den Grenzzustand der Gebrauchstauglichkeit.

Die Auswertungsmethoden für Drucksondierungen basieren meist auf empirischen Korrelationen mit theoretischem Hintergrund. Die Datenintegration mit anderen, zusätzlichen Untersuchungstechniken wie Bohrungen und Laborversuchen erhöht den Grad der Zuverlässigkeit. Lunne et al. (1997) geben einen Überblick über verschiedene Auswertungsmethoden.

Die unten erläuterten Bewertungsmethoden unterliegen einigen Einschränkungen:

- Empirische Korrelationen beziehen sich auf Referenzparameter, welche in einem festgelegten Referenzverfahren gemessen wurden. So bezieht sich die mit einem N_{kT}-Faktor von Sondierergebnissen abgeleitete undrainierte Scherfestigkeit auf denen, welche in einem einstufigen, isotrop konsolidierten, undrainierten Triaxialversuch (CIU) an einer ungestörten Bodenprobe im Labor ermittelt wurde. Der Bezugsparameter ist nicht unbedingt dem gewählten geotechnischen Modell angemessen, so dass eine Anpassung erforderlich sein könnte.
- Die meisten Bewertungsmethoden gelten meistens für einen Sand oder einen Ton. Bei Silt, Ton/Sand/Kies Mischungen, sehr dünn geschichteten Böden, zementierten Schichten und/oder Verwitterungsböden kann es zu Abweichungen kommen. Im Falle von solchen Schichten muss spezifisch vorgegangen werden (Peuchen et al., 1996; Lunne et al., 1995).
- Die Auswertungen beziehen sich auf die Bedingungen zu Beginn der geotechnischen Untersuchungen. Geologische und umwelttechnische Faktoren sowie Bauarbeiten können die vorgefundenen Baugrundverhältnisse verändern.
- Die Drucksondierung gibt nur bedingt direkte Information über den Grenzzustand der Gebrauchstauglichkeit (Verformungen), da beim Eindringen der umliegende Boden stark deformiert wird. Im Vergleich zum Grenzzustand der Tragfähigkeit können genauere zusätzliche Daten erforderlich sein.

- Drainiertes oder undrainiertes Verhalten für die geotechnische Analyse kann dem jeweiligen drainierten oder undrainierten Verhalten während dem Sondiervorgang entsprechen, muss dies aber nicht. Es ist Aufgabe des Geotechnik-Ingenieurs zu beurteilen, welches Verhalten für die geotechnische Fragestellung relevant ist.

EINDRINGVERHALTEN

Während des Sondiervorgangs treten grössere Deformationen in unmittelbarer Nähe, und kleinere elastische Deformationen in grösserem Abstand des Penetrometers auf. Die Zusammensetzung der einzelnen Schichten, die Lagerungsdichte, die Struktur und die In-Situ Spannungsverhältnisse beeinflussen die Messgrössen.

Der gemessene Spitzenwiderstand q_c wird unter anderem durch den Porenwasserdruck beeinflusst. Da das Verhältnis effektiver Spannung zum Porendruck in grobkörnigen Schichten hoch ist, kann dieser Einfluss normalerweise vernachlässigt werden. Beim Eindringen in Ton ist dasselbe Verhältnis jedoch niedrig. Es kann somit wichtig sein zu wissen, wie hoch der Porendruck um das Penetrometer herum ist. Zu den Parametern, die die Auswirkungen des Porendrucks berücksichtigen, zählen der Gesamtspitzenwiderstand q_t, der Netto-Spitzenwiderstand q_n und das Porendruckverhältnis B_q. Diese Parameter können berechnet werden, wenn Daten bezüglich des Porenwasserdrucks vorliegen. Die Auswirkungen des Porendrucks auf die Mantelreibung f_s sind sehr gering und werden üblicherweise ignoriert. Die Berechnung des Reibungsverhältnisses R_f (definiert als f_s/q_c) lässt keine Rückschlüsse auf die Auswirkungen des Porendrucks zu.

Die Eindringgeschwindigkeit in Bezug auf die Durchlässigkeit des Bodens bestimmt, ob das Bodenverhalten in erster Linie undrainiert, drainiert oder teilweise drainiert ist. Normalerweise ist das Bodenverhalten bei Drucksondierungen in Sand und Kies drainiert (es gibt keinen messbaren, aufgrund des Sondiervorgangs hervorgerufenen Porenwasserdruck) und in Ton undrainiert (bedeutende Änderung des Porenwasserdrucks). Teilweise drainiert ist es bei Böden mit mittlerer Durchlässigkeit, wie z. B. bei Silt. Die folgenden Abschnitte gehen näher auf die Ermittlung von geotechnischen Parametern aufgrund von elektrischen Drucksondierungen ein.

KLASSIFIZIERUNG

Die Klassifizierung der verschiedenen Schichten in Bezug auf das allgemeine Bodenverhalten (und in eingeschränkterem Masse die Bodenart) ist, im Vergleich mit anderen Ermittlungstechniken, ein wichtiger Teil der Drucksondierung.

Die Klassifizierung des Bodenverhaltens steht im Einklang mit der von Robertson (1990) beschriebenen Vorgehensweise. Diese betrachtet eine normalisierte Klassifizierung des Bodenverhaltens, die eine allgemeine Leitlinie zur Bestimmung der wahrscheinlichen Bodenart (z. B. Sand, siltig) gibt. Hierzu sind Daten einer Porenwasserdrucksondierung nötig. Es besteht eine vereinfachte Vorgehensweise für Ergebnisse ohne Messung des Porenwasserdrucks (Robertson et al., 1986).

IN-SITU SPANNUNGSVERHÄLTNISSE

Die Spannungsverhältnisse im Baugrund müssen bekannt sein, damit Parameter wie die bezogene Lagerungsdichte I_D und der innere Reibungswinkel φ' ermittelt werden können. Die effektive vertikale Spannung σ'_v kann berechnet werden, jedoch ist die effektive horizontale Spannung $\sigma'_{ho} = K_o\sigma'_{vo}$ meist unbekannt und hängt primär vom Überkonsolidierungsgrad OCR [-] und dem effektiven inneren Reibungswinkel φ' [°] ab:

$$K_0 = (1 - \sin \varphi') \cdot OCR^{\sin \varphi'} \quad [1]$$

Für eine Erklärung der verwendeten Symbole siehe Anhang „elektrische Drucksondierung (CPT)“, insofern nicht anders erwähnt. Der Zusammenhang basiert auf mechanischer Überkonsolidierung von rekonstituierten Probekörpern im Labor. Überkonsolidierung kann in der Natur durch geologische Faktoren wie z.B. glaziale Vorbelastung und Erosion, aber auch durch Grundwasserschwankungen und das Altern der Ablagerungen („ageing“) hervorgerufen werden. Normalerweise bewegen sich In-Situ Werte für K_o für Tiefen bis zu 50 m zwischen 0.4 und 2.0. In grösseren Tiefen (> 50 m) beträgt dieser Ruhedruckkoeffizient üblicherweise weniger als 1.

Der maximale passive Erddruck stellt eine Obergrenze für die effektive horizontale Spannung dar. Der Koeffizient des passiven Erddrucks richtet sich unter Vernachlässigung einer allfälligen Kohäsion nach:

$$K_p = \frac{1 + \sin \varphi'}{1 - \sin \varphi'} \quad [2]$$

Wenn die effektive horizontale Spannung das Niveau des passiven Erddrucks erreicht, können Risse im Erdreich entstehen. In ausgetrockneten Tonen kann auch früher Rissbildung auftreten. In verkitteten Schichten kann aufgrund der vorhandenen Kohäsion ein horizontaler Erddruck vorhanden sein, welcher grösser ist als oben beschrieben. Die Kombination der Beziehung für K_0 und K_p ergibt eine Obergrenze für die Überkonsolidierung:

$$OCR_{max} = \left[\frac{1 + \sin \varphi'}{(1 - \sin \varphi')^2} \right]^{\frac{1}{\sin \varphi'}} \quad [3]$$

Für einen Ton kann der maximale Überkonsolidierungsgrad OCR_{max} somit weniger als 4, für einen Sand jedoch mehr als 50 betragen.

Der Überkonsolidierungsgrad von feinkörnigen Sedimenten kann direkt aus den Sondierergebnissen abgeleitet werden (Kulhawy und Mayne, 1990):

$$OCR = \alpha \cdot (q_T - \sigma_v) \quad [4]$$

Kulhawy und Mayne schlagen einen α-Wert von 0.3 [-] vor. Die Korrelation von elektrischen Drucksondierungen mit ausgewerteten Oedometer-Versuchen für Tone und Silte in der Schweiz suggeriert, dass ein Wert von 0.25 den Schweizer Verhältnissen besser angemessen sein dürfte. Geoprofile GmbH legt der Abschätzung des Überkonsolidierungsgrades (OCR) einen α-Wert von 0.25 zugrunde, was im Vergleich zu Kulhawy und Mayne zu einem etwas tieferen Überkonsolidierungsgrad führt.

Für Sande und Kiessande kann der Überkonsolidierungsgrad wie folgt abgeschätzt werden:

$$OCR = \left[\frac{0.192 \cdot (q_t / p_{atm})^{0.22}}{(1 - \sin \varphi')(\sigma'_{vo} / p_{atm})^{0.31}} \right]^{\frac{1}{\sin \varphi' - 0.27}}$$

wobei p_{atm} den atmosphärischen Druck bezeichnet.

Der maximale Vorkonsolidierungsdruck σ'_p ergibt sich aus der Multiplikation mit der effektiven vertikalen Spannung In-Situ:

$$\sigma'_p = \sigma'_{vo} \cdot OCR \quad [5]$$

Wird zudem der effektive innere Reibungswinkel φ' ermittelt, ist gemäss [1] auch der horizontale Erdruhedruck bekannt.

EFFEKTIVE SCHEREIGENSCHAFTEN

Der effektive innere Reibungswinkel φ' ist keine Konstante. Er hängt neben der Zusammensetzung (Mineralogie, Kornform und -rauheit) und der Lagerungsdichte zudem von den Spannungsverhältnissen im Erdreich und dem Abschermodus ab. Es gibt Hinweise dafür, dass Faktoren wie der Sedimentationsmodus oder die In-Situ Spannungsanisotropie weniger von Bedeutung sind.

Die ermittelten Werte der effektiven Reibungswinkel beziehen sich auf das In-Situ Spannungsniveau während der Sondierung. Dies dürfte z.B. für die Berechnung der Stabilität einer Böschung angemessen sein. Im Falle einer signifikanten Erhöhung der Spannungsverhältnisse, wie z.B. bei einer Aufschüttung oder einer Pfahlgründung, muss der effektive Reibungswinkel für Sand und Kiessand den neuen Verhältnissen angepasst werden, was meistens eine Verringerung der Scherparameter bedeutet. Das Verfahren nach Bolton (1986, 1987) stellt dazu eine breit akzeptierte Methode dar. Da der kritische Reibungswinkel φ'_{krit} im Falle von feinkörnigen Böden bereits bei einem geringen Spannungsniveau erreicht wird, ist die Abstufung von effektiven Scherparametern für Ton und Silt weniger üblich.

Das Verhältnis des inneren Reibungswinkels φ' zum Spitzenwiderstand q_c kann auf mehr oder weniger aufwendige Art und Weise ermittelt werden. Einfache Vorgehensweisen stützen sich auf eine konservative Klassifizierung des Bodenverhaltens. Eine aufwendigere empirische Untersuchung berücksichtigt zudem die In-Situ Spannungsverhältnisse σ'_{vo} und σ'_{ho} (siehe Abschnitt „In-Situ Spannungsverhältnisse“). Zudem kann die Lagerungsdichte explizit miteinbezogen werden. Neuere Ansätze verzichten jedoch darauf und berücksichtigen die Lagerungsdichte mit dem Einbezug von q_c nur implizit, da bei der Abschätzung der Lagerungsdichte zusätzliche Unsicherheiten eingebracht werden.

Eine Überprüfung der Ergebnisse von Drucksondierungen in mit Sand gefüllten Kalibrationskammern erlaubt die Abschätzung des effektiven inneren Reibungswinkels φ’ für dieses Material (Kulhawy und Mayne, 1990):

$$\varphi' = 17.6 + 11 \cdot \log(q_{t1}) \qquad [6]$$

$$q_{t1} = \frac{q_t / p_{atm}}{\sqrt{\sigma'_{vo} / p_{atm}}} \qquad [p_{atm} = \text{atmosphärischer Druck} \approx 100\ \text{kPa}] \qquad [7]$$

Als Referenzverfahren gelten axial belastete Triaxialprüfungen von isotrop und anisotrop konsolidierten Sandproben (CID unf CAD). Die Korrelation enthält im Vergleich zu früheren Gleichungen (z.B. Robertson und Campanella, 1983) eine Korrektur für die Grösse der Kalibrationskammer im Vergleich zur Sondierspitze.

Die Abschätzung der effektiven Scherparameter für fein- und gemischtkörnige Ablagerungen beruht auf einer Form der Tragfähigkeitsformel (Senneset et al., 1988, 1989):

$$q_n = N_m(\sigma'_{vo} + a) \quad [9]$$

wobei:

$$N_m = \frac{N_q - 1}{1 + N_u B_q} \quad [10]$$

$$N_q = \tan^2(45 + \tfrac{1}{2}\varphi')e^{(\pi - 2\beta)\tan\varphi'} \quad [11]$$

$$N_u = 6\tan\varphi'(1 - \varphi') \quad [12]$$

β = Plastifizierungswinkel

a = Anziehung

Dazu muss der Plastifizierungswinkel und die Anziehung („attraction“) abgeschätzt werden. Senneset et al. geben Richtwerte für verschiedenen Materialen als Funktion der Konsistenz bzw. der Lagerungsdichte. Die Abschätzung des effektiven inneren Reibungswinkels ist relativ unabhängig von den gewählten Werten für β und a. Die von Geoprofile gewählte Vorgehensweise basiert auf einer vorsichtigen Schätzung der beiden Parameter.

Die Abschätzung der effektiven Kohäsion für feinkörnige Schichten richtet sich nach dem maximalen Vorkonsolidierungsdruck σ'_p (Mesri und El-Ghaffar, 1993):

$$c' = 0.024 \cdot \sigma'_p \quad [13]$$

Für die Bestimmung des maximalen Vorkonsolidierungsdrucks σ'_p siehe den Abschnitt „In-Situ Spannungsverhältnisse“. Die Integration von weiteren geotechnischen Datensätzen für die Ermittlung der effektiven Kohäsion ist empfehlenswert. Ob die Anwendung einer effektiven Kohäsion hinsichtlich der geotechnischen Fragestellung und dem nicht-linearen Verlauf der Einhüllende sinnvoll ist, muss durch einen Geotechnik-Ingenieur beurteilt werden. Für Langzeit-Analysen kann es angebracht sein, die effektive Kohäsion vollständig zu vernachlässigen.

BEZOGENE LAGERUNGSDICHTE

Die Bestimmung des minimalen und des maximalen Porenraums der Sandproben im Labor (e_{min} und e_{max}) bildet die Grundlage für den Begriff der bezogenen Lagerungsdichte. Es ist unwahrscheinlich, dass bei den Laborversuchen tatsächlich der niedrigsten oder der höchsten Wert für den Porenraum e_{max} bzw. e_{min} ermittelt wird. Das In-Situ Raumgewicht kann somit den im Labor erfassten Wert übertreffen.

Übliche Zusammenhänge zwischen q_c und der bezogenen Lagerungsdichte I_D basieren auf Drucksondierungen in einer mit Sand gefüllten Kalibrationskammer. Derartige Versuche sind Teil von allgemeinen geotechnischen Forschungsprojekten und unterliegen einigen Beschränkungen, wie z. B.:

- Abhängigkeit von der Bodenart
- Ungenauigkeiten bei der Bestimmung von I_D im Labor
- begrenzte Bandbreite an Spannungshöhen und K_o Werten
- Vereinfachungen bei der Probenvorbereitung und den Aufzeichnungen zur Bodenspannung

Folgende Schritte dienen zur Bestimmung der Lagerungsdichte (locker, dicht, etc.) vor Ort:

(a) Schätzung der In-Situ Spannungsverhältnisse σ'_{vo} und σ'_{ho}

(b) Empirische Korrelation der bezogenen Lagerungsdichte I_D mit q_c, σ'_{vo} und σ'_{ho}

Die Abschätzung der In-Situ Spannungsverhältnisse wurde oben erläutert. Sind zudem allgemeine Angaben zur Kompressibilität des Sands vorhanden, sollten diese in die Beurteilung der bezogenen Lagerungsdichte miteinbezogen werden. Die Kompressibilität eines Sands nimmt tendenziell zu mit zunehmender Uniformität der Korngrösseverteilung, mit der Eckigkeit der einzelnen Körner und mit zunehmendem Feinanteil.

Die Abschätzung der bezogenen Lagerungsdichte richtet sich nach Kulhawy und Mayne (1990):

$$I_D^{\,2} = \frac{q_{t1}}{305\ Q_c \cdot Q_{OCR} \cdot Q_A} \qquad [14]$$

wobei q_{t1} sich nach [7] richtet und die Faktoren Q_c, Q_{OCR} und Q_A wie folgt berechnet werden:

Q_c = Kompressibilitätsfaktor
$0.91 < Q_c < 1.09$ (Tiefer Wert für geringe Kompressibilität)

Q_{OCR} = Überkonsolidierungsfaktor
$OCR^{0.2}$

Q_A = Faktor, welche die Zunahme des Spitzenwiderstands mit der Zeit berücksichtigt
$1.2 + 0.05 \cdot \log(t/100)$ (t in Jahren)
≈ 1.3 für Sande, welche nach der letzten Eiszeit abgelagert wurden

ZUSAMMENDRÜCKUNGSMODUL BEI ERSTBELASTUNG

Zusammenhänge zwischen den Resultaten von Drucksondierungen und dem eindimensionalen Zusammendrückungsmodul bei Erstbelastung M_{E1} sind indikativ. Für eine genaue Bestimmung des Last-Deformationsverhaltens sind zusätzliche Daten (z. B. Plattendilatometer, Oedometerprüfung) unumgänglich.

Normalerweise wird die Elastizitätstheorie für die Analyse des Verformungsverhaltens von drainierten Böden angewandt. Lunne und Christophersen (1983) schlagen aufgrund einer Überprüfung der Ergebnisse von Drucksondierungen in mit Sand gefüllten Kalibrationskammern die folgende Beziehung zur Abschätzung des Zusammendrückungsmoduls bei Erstbelastung vor:

$$M_{E1} = \begin{cases} 4 \cdot q_c & q_c < 10 \text{ MPa} \\ 2 \cdot q_c + 20 & 10 < q_c < 50 \text{ MPa} \\ 120 & q_c > 50 \text{ MPa} \end{cases} \quad [15]$$

Die Abschätzung des eindimensionalen Zusammendrückungsmoduls bei Erstbelastung für feinkörnige Schichten richtet sich meistens nach:

$$M_{E1} = \alpha_c \cdot q_c \quad [16]$$

Oder, korrigiert für den transienten Porenwasserdruck und den Bau der Messsonde:

$$M_{E1} = \alpha_n \cdot q_n \quad [17]$$

Dabei stellt α einen Korrelationskoeffizient dar, welcher unter anderem von der Plastizität, Korngrösse, Mineralogie und Spannungsgeschichte abhängt. Mitchell und Gardner (1975) geben Richtwerte für α_c, welche sich je nach Zusammensetzung, Plastizität und Scherfestigkeit zwischen 1 und 8 bewegen. Neuere Studien aufgrund des netto Spitzenwiderstands q_n empfehlen einen Wert für α_n zwischen 4 und 8 (Senneset et al, 1989). Die von Geoprofile gewählte Methode betrachtet einen pauschalen Wert für α_n von 5 als praktikabel.

Der hier abgeleitete Zusammendrückungsmodul ist einen oedometrischen Modul, welche sich auf die effektiven in-situ Spannungsverhältnisse in einer bestimmten Tiefe bezieht. Bei der Bestimmung eines Zusammendrückungsmoduls beim Oedometerversuch gilt, dass die vertikalen Dehnungen sehr gross sind und meistens zwischen 1 und 10 Prozent variieren. Solche Dehnungen sind unter einem Bauwerk kaum realistisch. Es liegt in der Verantwortung des Anwenders, die effektiv auftretenden Dehnungen bei der Wahl eines geeigneten M_E-Wertes gebührend zu berücksichtigen. Dies kann durchaus zu einem höheren Wert führen. Die Verwendung eines konstanten, oedometrischen Zusammendrückungsmoduls führt bei Setzungsberechnungen in der Regel zu einer Überschätzung der zu erwartenden Setzungen.

Zur Berücksichtigung einer grösseren Steifigkeit des Baugrundes bei geringeren Dehnungen sollte vorzugsweise auf komplexeren Materialmodellen zurückgegriffen werden (z.B. das hardening soil small strain Modell (HSS)).

Die Abschätzung der maximalen Vorkonsolidierungsspannung σ'_p richtet sich nach [5].

UNDRAINIERTE SCHERFESTIGKEIT

Die undrainierte Scherfestigkeit s_u ist keine Konstante. Sie hängt von Faktoren wie dem Abschermodus und der -richtung, der Spannungshistorie und –anisotropie sowie der Abschergeschwindigkeit und der Temperatur ab.

Es gibt verschiedene theoretische und empirische Vorgehensweisen, um den Spitzenwiderstand q_c mit der undrainierten Scherfestigkeit s_u zu korrelieren. Theoretische Ansätze stützen sich auf die Tragfähigkeitstheorie oder die Bodenmechanik des kritischen effektiven Zustands (critical state soil mechanics, CSSM). So kann der einfache Abschermodus wie folgt beschrieben werden (Wroth 1984):

$$s_u / \sigma'_{vo\ DDS} = \tfrac{1}{2} \sin \varphi' \cdot OCR^{\Lambda} \qquad [18]$$

wobei $\Lambda = 1\text{-}C_s/C_c$ das plastische volumetrische Dehnungspotential, und C_c und C_s den Zusammendrückungsindex bei Erstbelastung bzw. bei Entlastung bezeichnen. Für Tone mit einer geringen bis mittleren Sensitivität liegt Λ meistens zwischen 0.7 und 0.8, für sensitive Tone eher um 0.9. Die bekannte Beziehung (Jamiolkowski et al., 1985; Ladd, 1991; Ladd and DeGroot 2003):

$$s_u / \sigma'_{vo\ DDS} = 0.22 \cdot OCR^{0.8} \qquad [19]$$

welche im Erdbaulabor des MIT entwickelt wurde, ist dabei ein Subsatz von [18] mit $\varphi' = 26^o$ und $\Lambda = 0.8$. Die von Geoprofile gewählte Methode nutzt den aus den Sondierdaten abgeleiteten Wert für den effektiven inneren Reibungswinkel φ' und einem Λ von 0.8.

Empirische Ansätze beruhen meistens auf einer direkten Korrelation des netto Spitzenwiderstands q_n mit der undrainierten Scherfestigkeit (Rad und Lunne, 1988):

$$s_{u\ TX} = \frac{q_t - \sigma_{vo}}{N_{kt}} = \frac{q_n}{N_{kt}} \qquad [20]$$

Der Faktor N_{kt} liegt üblicherweise zwischen 15 und 25, hängt aber unter anderem von der Plastizität und

dem Überkonsolidierungsgrad ab. Das Referenzverfahren für die oben genannte Beziehung ist der konsolidierte, undrainierte, triaxiale Zusammendrückungstest (CU). Die von Geoprofile gewählte Vorgehensweise bezieht sich auf eine undrainierte Scherfestigkeit mit einem Faktor N_{kt} von 18, welche aber nur zur Kontrolle von der mit [18] abgeleiteten undrainierte Scherfestigkeit (und damit indirekt auch von φ') herangezogen wird.

Die Sensitivität eines Tons ist das Verhältnis zwischen der maximalen und der gestörten undrainierten Scherfestigkeit:

$$S_t = s_{u,max} / s_{u,rest} \quad [21]$$

Da die gemessene lokale Mantelreibung f_s in Ton primär von der gestörten undrainierten Scherfestigkeit abhängt, kann die Sensitivität wie folgt abgeleitet werden Rad und Lunne, 1986):

$$S_t = \frac{N_s}{R_f} \quad [22]$$

wobei R_f das Reibungsverhältnis bezeichnet und N_s üblicherweise zwischen 6 und 9 liegt. Bei der von Geoprofile gewählten Vorgehensweise liegt der Abschätzung der Sensitivität ein Wert für N_s von 7.5 zugrunde.

LITERATURANGABEN

Bolton, M.D. (1986), "The Strength and Dilatancy of Sands", Geotechnique, Vol. 36, No. 1, pp. 65-78.

Bolton, M.D. (1987), "The Strength and Dilatancy of Sands, Discussion", Geotechnique, Vol. 37, No. 2, pp. 225-226.

Kulhawy, F.H. und P.W. Mayne, (1990), Manual on Estimating Soil Properties for Foundation Design, Report EPRI EL-6800, Electric Power Research Institute, Palo Alto, California, 306 pp.

Ladd, C.C., Foott, R.R., Ishihara, K., Schlosser, F. und Poulos, H.G. (1977), "Stress-Deformation and Strength Characteristics", Proc. 9th Int. Conf. on Soil Mechanics and Foundation Engineering, Tokyo, Vol. 2, pp. 421-494.

Lunne, T., Powell, J.J.M. und Robertson, P.K. (1995), "Use of Piezocone Tests in Non-Textbook Materials", Proc. Int. Conf. on Advances in Site Investigation Practice, Institution of Civil Engineers, London, pp. 438-451.

Lunne, T und Christophersen, H.P. (1983), "Interpretation of cone Penetrometer data for offshore Sands", Proc. of the offshore technology conference, Richardson, Texas, paper nr. 4464

Lunne, T., Robertson, P.K. und Powell, J.J.M. (1997), "Cone Penetration Testing in Geotechnical Practice", Blackie Academic & Professional, London, p. 312.

Mayne, P.W. und Kulhawy, F.H. (1982), "K_o - OCR Relationships in Soil", ASCE Jnl. of Geotechnical Engineering, Vol. 108, No. GT6, pp. 851-872.

Mesri, G. und Abdel-Ghaffar, M.E.M. (1993). "Cohesion Intercept in Effective Stress Stability Analysis." Journal of Geotechnical Engineering, Vol. 119, No. 8, pp. 1229-1249.

Mitchell, J.K. und Gardner, W.S. (1975), "In-Situ Measurements of Volume Change Characteristics", ASCE Speciality Conference on In-Situ Measurement of Soil Properties, North Carolina, Vol. II, pp. 279-345.

Rad, N.S. und Lunne, T. (1988), "Direct Correlations between Piezocone Test Results and Undrained Shear Strength of Clay", Penetration Testing 1988, Proc. First Int. Symp. On Penetration Testing, ISOPT-1, De Ruiter (ed.), Vol. 2, pp. 911-917.

Robertson, P.K. (1990), "Soil Classification using the Cone Penetration Test", Can. Geotech. Jnl., Vol. 27, No. 1, pp. 151-158.

Robertson, P.K., Campanella, R.G., Gillespie, D. und Grieg, J. (1986), "Use of Piezometer Cone Data", Proc. In-Situ '86, ASCE Specialty Conf., Blacksburg, VA, pp. 1263-1280.

Senneset, K., R. Sandven, T. Lunne, T. By, und T. Amundsen, (1988), “Piezocone Tests in Silty Soils,” Penetration Testing, Vol. 2, Balkema, Rotterdam, The Netherlands, pp. 955–974.

Senneset, K., R. Sandven, und N. Janbu, (1989), “Evaluation of Soil Parameters from Piezocone Tests,” Transportation Research Record 1235, Transportation Research Board, National Research Council, Washington, D.C, pp. 24–37.

Wroth, C.P. (1984), "The Interpretation of In-Situ Soil Tests", Geotechnique, Vol. 34, No. 4, pp. 449-489.

Performance based earthquake design using the CPT

P.K. Robertson
Gregg Drilling & Testing Inc., Signal Hill, California, USA

ABSTRACT: Application of the Cone Penetration Test (CPT) for the evaluation of seismic performance is reviewed and updates presented. The role of the CPT in geotechnical earthquake engineering is presented. The use of the CPT to identify soil behavior type and the normalization of CPT parameters is also reviewed and updates presented. The case-history based method to evaluate the resistance of sand-like soils to cyclic loading is reviewed and compared with the expanded and re-evaluated case history database. The laboratory based method to evaluate the resistance of clay-like soils to cyclic loading is reviewed and modified for application using the CPT. A new combined CPT-based method to evaluate the resistance to cyclic loading is proposed that covers all soils and is evaluated using an expanded case history database. The CPT-based method is extended to estimate both volumetric and shear strains for all soils and evaluated using the expanded case history database.

1 INTRODUCTION

The seismic performance of geotechnical structures often requires an estimate of potential post-earthquake displacements. Historically, geotechnical earthquake design has focused extensively on evaluation of liquefaction in sandy soils since deformations tend to be large when soils experience liquefaction. Liquefaction analyses have traditionally focused on the evaluation of factor of safety and using this as an indicator of potential post-earthquake deformations. Recently there has been growing awareness that soft clays can also deform during earthquake loading.

In North American building codes (e.g. NBC 2005, FEMA 356 and SEAOC 1995), the design philosophy for earthquake loading is to accept some level of damage to structures, i.e. to accept some level of deformation. The acceptable level of damage and deformation is a function of the importance of the structure and the earthquake return period. The importance of the structure is a function of the risk. The evaluation of post-earthquake deformations is therefore a key element in any performance based earthquake design.

Due to size limitations, this paper will only discuss the application of the Cone Penetration Test (CPT) for the evaluation of post-earthquake deformations. The intent of this paper is not to imply that all earthquake geotechnical design can be accomplished using only the CPT; other in-situ tests along with sampling and laboratory testing also play a role, depending on the risk of the project.

2 ROLE OF CPT IN GEOTECHNICAL EARTHQUAKE ENGINEERING

Since this paper is focused on the application of CPT results for the evaluation of post-earthquake deformations, it is appropriate to briefly discuss the role of the CPT in geotechnical earthquake engineering practice. Hight and Leroueil (2003) suggested that the appropriate level of sophistication for a site characterization and analyses program should be based on the following criteria:

- Precedent and local experience
- Design objectives
- Level of geotechnical risk
- Potential cost savings

The evaluation of geotechnical risk was described by Robertson (1998) and is dependent on hazards (what can go wrong), probability of occurrence (how likely is it to go wrong) and the consequences (what are the outcomes). Earthquake loading can be a significant hazard, but the resulting risk is primarily a

function of the probability of occurrence and the consequences. General recommendations for the appropriate level of sophistication for site investigation and subsequent design can be summarized in Table 1. Although Table 1 indicates only two broad outcomes, Robertson (1998) and Lacasse and Nadim (1998) showed that the level of risk cover a range from low to high and that the resulting site characterization program should vary accordingly.

For low risk projects, traditional methods, such as in-situ logging tests (e.g. CPT, SPT) and index testing on disturbed samples combined with conservative design criteria, are often appropriate. For the evaluation of liquefaction and post earthquake deformations the Simplified Procedure, first proposed by Seed and Idriss (1971) and recently updated by Youd et al. (2001), is appropriate for low risk projects. For moderate risk projects, the Simplified Procedure should be supplemented with additional specific in-situ testing where appropriate, such as seismic CPT with pore pressure measurements (SCPTu) and field vane tests (FVT) combined with selective sampling and basic laboratory testing to develop site specific correlations. Sampling and laboratory testing is often limited to fine-grained soils where conventional sampling is easier and appropriate. For high risk projects, the Simplified Procedure can be used for screening to identify potentially critical regions/zones appropriate to the design objectives. This should be followed by selective high quality sampling and advanced laboratory testing. The results of laboratory testing should be correlated to in-situ test results to extend the results to other regions of the project. The Simplified Procedure for liquefaction evaluation should be used only as a screening technique to identify potentially critical regions/zones for high risk projects. Advanced techniques, such as numerical modeling, are often appropriate for more detailed evaluation of potential post-earthquake deformations for high risk projects.

One reason for the continued application of the Standard Penetration Test (SPT) as a basic logging test is that the test provides a soil sample suitable for index testing, even though the test can be unreliable. A common complaint about the CPT is that it does not provide a soil sample. Although it is correct that a soil sample is not obtained during the CPT, most commercial CPT operators have a simple push-in soil sampler that can be pushed using the CPT installation equipment to obtain a small (typically 25 mm diameter) disturbed sample of similar size to that obtained from the SPT. Often the most cost effective solution is to obtain a detailed continuous stratigraphic profile using the CPT, then to move over a short distance (< 1m) and push a small diameter sampler to obtain discrete selective soil samples in critical layers/zones that were identified by the CPT. Continuous push samplers are also available to collect plastic-lined near continuous small diameter, disturbed soil samples. The push rate to obtain soil samples can be significantly faster than the 2 cm/s required for the CPT therefore making sampling rapid and cost effective for a small number of discrete samples. For low risk projects the efficiency and cost effectiveness of CPT, combined with adjacent discrete push-in soil samples, is usually superior to that of CPT plus adjacent boreholes with SPT.

Many of the comments and recommendations contained in this paper are focused on low to moderate risk projects where traditional (simplified) procedures are appropriate and where empirical interpretations tend to dominate. For projects where more advanced procedures are appropriate, the recommendations provided in this paper can be used as a screening to evaluate critical regions/zones where selective additional in-situ testing and sampling may be appropriate. Risk based site investigation and analysis is consistent with performance based design principles where the design criteria are in terms of deformation based on the risk of the structure.

Table 1 Appropriate level of sophistication for Site Characterization and Analyses

Rating	*Criteria*	*Rating*
GOOD	*Precedent & local experience*	POOR
SIMPLE	*Design objectives*	COMPLEX
LOW	*Level of geotechnical risk*	HIGH
LOW	*Potential for cost savings*	HIGH
LOW RISK PROJECT		HIGH RISK PROJECT
TRADITIONAL (simplified) METHODS		*ADVANCED (complex) METHODS*

3 BASIC SOIL BEHAVIOR UNDER EARTHQUAKE LOADING

Boulanger and Idriss (2004b, 2007) showed that, for practical purposes, soils can be divided into either 'sand-like' or 'clay-like' soils, where sand-like soils can experience 'liquefaction' and clay-like soils can experience 'cyclic failure'. In a general sense, sand-like soils are gravels, sands, and very-low plasticity silts, whereas clay-like soils are clays and plastic silts.

In general, all soils deform under earthquake loading. Earthquakes impose cyclic loading rapidly and soils respond undrained during the earthquake. In general, all soils develop some pore pressure during earthquake loading and at small strains these pore pressures are almost always positive. Sand-like soils can develop high positive pore pressures during undrained cyclic loading and can reach a condition of zero effective confining stress. At the condition of zero effective stress, the initial structure of the soil is lost and the stiffness of the soil in shear is essentially zero or very small and large deformations can occur during earthquake loading. The condition of zero effective stress is often defined as 'liquefaction' or 'cyclic liquefaction'. Loose, young, uncemented sand-like soils are more susceptible to 'liquefaction' than dense sand-like soils. The ability of sand-like soils to liquefy is a function of in-situ state (relative density and effective confining stress), structure (age, fabric and cementation) and the size and duration of the cyclic loading. Most liquefaction cases occur in young uncemented sand-like soils. During earthquake loading, loose sand-like soils can experience very large shear strains which can result in large lateral and vertical deformations, depending on ground geometry and external static loads (e.g. buildings, embankments, slopes, etc.). Very loose sand-like soils can also experience strength loss after earthquake loading that can result in flow slides with very large deformations depending on ground geometry and drainage. Following earthquake loading, sand-like soils can also experience volumetric strains and post-earthquake reconsolidation settlements. The resulting volumetric strains can be large due to the loss of initial soil structure at zero effective stress and resulting small volumetric stiffness (constrained modulus) during initial reconsolidation. These settlements generally occur rapidly after the earthquake (i.e. in less than a few hours), depending on soil stratigraphy and drainage conditions.

Clay-like (cohesive) soils can also develop pore pressures during undrained cyclic loading, but generally do not reach zero effective stress and hence retain some level of stiffness during cyclic loading and generally deform less than sand-like soils. Traditionally, clay-like soils are considered not susceptible to liquefaction, since they generally do not reach a condition of zero effective stress. However, clay-like soils can deform during cyclic earthquake loading. The amount of pore pressure buildup is a function of in-situ state (overconsolidation ratio), sensitivity, structure (age, fabric and cementation) and size and duration of cyclic loading. Soft normally to lightly overconsolidated and sensitive clay-like soils can develop large positive pore pressures with significant shear strains during earthquake loading that can result in lateral and vertical deformations, depending on ground geometry and external static loads (e.g. buildings, embankments, slopes, etc.). Very sensitive clay-like soils can also experience strength loss after earthquake loading that can result in flow slides with very large deformations depending on ground geometry. Following earthquake loading, clay-like soils can also experience volumetric strains and post-earthquake reconsolidation settlements. However, these settlements generally occur slowly after the earthquake due to the lower permeability of clay-like soils and are also a function of soil stratigraphy and drainage conditions. The volumetric strains during post earthquake reconsolidation are generally small since clay-like soils often retain some original soil structure and hence, maintain a high value of volumetric stiffness during reconsolidation.

Following earthquake loading, pore-water redistribution can result in some sand-like soils changing void ratio and becoming looser. This can result in strength loss and the potential for instability.

Recent research has indicated that the transition from sand-like to clay-like soils can be approximately defined by Atterberg Limits (e.g. plasticity index) of the soil (Seed et al, 2003; Bray and Sancio, 2006; Boulanger and Idriss, 2007). Sangrey et al. (1978) suggested that the transition was controlled by the compressibility of the soil, where, in general, clay-like soils have a higher compressibility than sand-like soils. In a general sense, soft normally consolidated clay-like fine grained soils respond in a similar manner to loose sand-like soils in that they are both contractive under shear and develop positive pore pressures in undrained shear. Highly sensitive clay-like soils are similar to very loose sand-like soils in that both can experience a large increase in pore pressure under undrained shear and can experience significant strength loss (i.e. strain soften). Stiff overconsolidated clay-like fine grained soils respond in a similar manner to dense sand-like soils in that

they both dilate under shear at high strains. Soil response in fine grained soils is controlled partly by the amount and type of clay minerals. The plasticity index is an approximate measure of the mineralogy of the soil, where the amount and type of clay mineral influences soil behavior.

Traditionally, the response of sand-like and clay-like soils to earthquake loading is evaluated using different procedures. It is common to first evaluate which soils are sand-like, and therefore susceptible to liquefaction based on grain size distribution and Atterberg Limits, and then to determine the factor of safety (FS_{liq}) against liquefaction. A key element in performance based geotechnical earthquake design is the evaluation of post-earthquake deformations. The challenge is to develop procedures that capture the correct soil response as soil transitions from primarily sand-like to clay-like in nature. The objective of this paper is to outline a possible unified approach for all soils using CPT results with the ultimate goal to evaluate possible post-earthquake deformations.

4 CPT SOIL BEHAVIOUR TYPE

One of the major applications of the CPT has been the determination of soil stratigraphy and the identification of soil type. This has been accomplished using charts that link cone parameters to soil type. Early charts using q_c and friction ratio (R_f) were proposed by Douglas and Olsen (1981), but the charts proposed by Robertson et al. (1986) have become popular. Initially these charts were based on empirical correlations, but theoretical studies have supported the general concepts. Robertson et al. (1986) and Robertson (1990) stressed that the charts were predictive of Soil Behaviour Type (SBT) since the cone responds to the mechanical behaviour of the soil and not directly to soil classification criteria based on grain-size distribution and soil plasticity. Fortunately, soil classification criteria based on grain-size distribution and plasticity often relate reasonably well to soil behaviour and hence, there is often good agreement between soil classification based on samples and SBT based on the CPT. Several examples can be given when differences arise between soil classification and SBT based on CPT. For example, a soil with 60% sand and 40% fines may be classified as 'silty sand' using the unified classification system. However, if the fines are composed of a highly active clay mineral with high plasticity, the soil behaviour may be controlled more by the clay and the SBT from the CPT will reflect this behaviour and predict a more clay-like behaviour, such as 'clayey silt'. If the fines were non-plastic the soil behaviour may be controlled more by the sand, the CPT SBT would predict a sand like soil type, such as 'silty sand'. Saturated loose silts often behave like soft clay in that their undrained strength is low and undrained response often governs geotechnical design. Hence, SBT based on CPT in soft saturated silts is often defined as clay. Very stiff heavily overconsolidated fine-grained soils tend to behave similar to coarse-grained soil in that they dilate at large strains under shear and can have high undrained shear strength compared to their drained strength. These few examples illustrate that the SBT based on the CPT may not always agree with traditional classification based on samples. Geotechnical engineers are usually interested in the behaviour of the soil rather than a classification based only on grain-size distribution and plasticity, although knowledge of both is useful.

The corrected cone (tip) resistance (q_t) responds to the average shear strength (depending on soil sensitivity, heterogeneity and macro fabric) of the soil ahead and behind the advancing cone, whereas the sleeve friction (f_s) and measured pore pressure (u_2) responds to the larger strain behaviour of the soil in contact with the cone. There is also a small scale effect and physical offset between the q_t and f_s measurements. Typically most commercially available CPT data acquisition systems adjust the two readings to present them at the same depth in the soil profile (i.e. the f_s reading is recorded when the center of the sleeve has reached the same depth/elevation as the cone tip). Soils with gravel particles can produce rapid unrepresentative variations in sleeve friction due to large particles touching the friction sleeve.

Robertson (1990) updated the CPT SBT charts using normalized (and dimensionless) cone parameters, Q_{t1}, F, B_q, where:

$$Q_{t1} = (q_t - \sigma_{vo})/\sigma'_{vo} \quad (1)$$

$$F_r = [(f_s/(q_t - \sigma_{vo})] \, 100\% \quad (2)$$

$$B_q = \Delta u / (q_t - \sigma_{vo}) \quad (3)$$

where:
σ_{vo} = pre-insertion in-situ total vertical stress
σ'_{vo} = pre-insertion in-situ effective vertical stress
u_0 = in-situ equilibrium water pressure
Δu = excess penetration pore pressure.

In the original paper by Robertson (1990) the normalized cone resistance was defined using the term Q_t. The term Q_{t1} is used here to show that the

cone resistance is the corrected cone resistance, q_t with the stress exponent for stress normalization n = 1.0. Note that in clean sands, $q_c = q_t$, but the more correct q_t is used in this paper.

In general, the normalized charts provide more reliable identification of SBT than the non-normalized charts, although when the in-situ vertical effective stress is between 50 kPa to 150 kPa there is often little difference between normalized and non-normalized SBT. The term SBTn will be used to distinguish between normalized and non-normalized SBT. Robertson (1990) suggested two charts based on either $Q_{t1} - F_r$ or $Q_{t1} - B_q$ but recommended that the $Q_{t1} - F_r$ chart was generally more reliable, especially for onshore geotechnical investigations where the CPT pore pressure results are more problematic and less reliable.

Jefferies and Davies (1993) identified that a Soil Behaviour Type Index, I_c, could represent the SBTn zones in the $Q_{t1} - F_r$ chart where I_c is essentially the radius of concentric circles that define the boundaries of soil type. Robertson and Wride (1998) modified the definition of I_c to apply to the Robertson (1990) $Q_{t1} - F_r$ chart, as defined by:

$$I_c = [(3.47 - \log Q_{t1})^2 + (\log F_r + 1.22)^2]^{0.5} \quad (4)$$

Contours of I_c are shown in Figure 1 on the Robertson (1990) $Q_{t1} - F_r$ SBTn chart. The contours of I_c can be used to approximate the SBT boundaries.

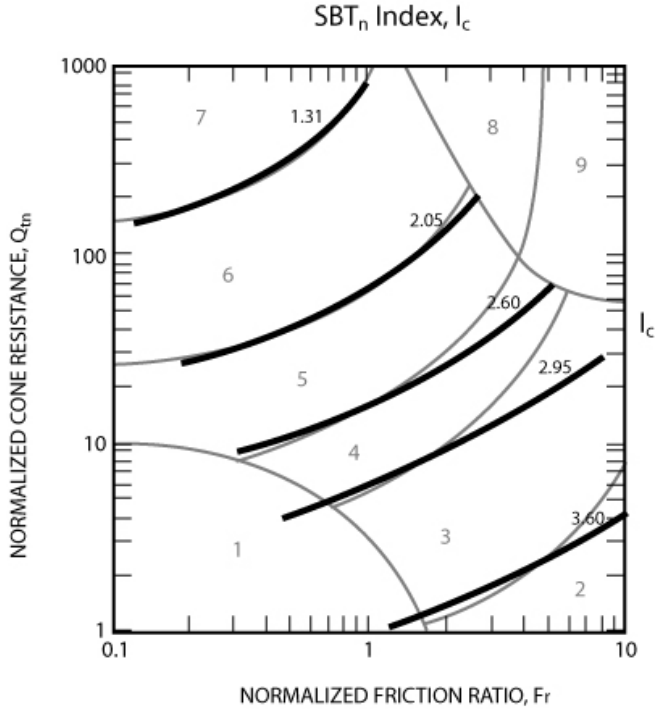

Figure 1. Contours of Soil Behaviour Type Index, I_c on normalized SBT Q_{tn}- F_r chart

Jefferies and Davies (1993) suggested that the SBT index I_c could also be used to modify empirical correlations that vary with soil type. This is a powerful concept and has been used where appropriate in this paper.

Robertson and Wride (1998) and updated by Zhang et al. (2002) suggested a normalized cone parameter, using normalization with a variable stress exponent, n, where:

$$Q_{tn} = [(q_t - \sigma_v)/p_a](p_a/\sigma'_{vo})^n \quad (5)$$

where:
$(q_t - \sigma_v)/p_a$ = dimensionless net cone resistance,
$(p_a/\sigma'_{vo})^n$ = stress normalization factor
n = stress exponent that varies with SBTn
p_a = atmospheric pressure in same units as q_t and σ_v.

Robertson and Wride (1998) and Zhang et al (2002) use the term, q_{c1N} instead of Q_{tn}. This paper will use the more general term, Q_{tn}. Where the term 'Q_t' denotes normalized corrected cone resistance and the subscript 'n' denotes normalization with a variable stress exponent. Note that, when n = 1, $Q_{tn} = Q_{t1}$. Zhang et al. (2002) suggested that the stress exponent, n, could be estimated using the SBTn Index, I_c, and that I_c should be defined using Q_{tn}.

Robertson (2008) recently updated the stress normalization by Zhang et al. (2002) to allow for a variation of the stress exponent with both SBTn I_c and effective overburden stress using:

$$n = 0.381\ (I_c) + 0.05\ (\sigma'_{vo}/p_a) - 0.15 \quad (6)$$

where $n \leq 1.0$

Robertson (2008) suggested that the above modification to the stress exponent would capture the correct state response for soils at high stress level and would avoid the need for a further stress level correction (K_σ) in liquefaction analyses.

There have been several publications regarding the appropriate stress normalization (Olsen and Malone, 1988; Robertson, 1990; Jefferies and Davies, 1991; Robertson and Wride, 1998; Zhang et al., 2002; Boulanger and Idriss, 2004a; Moss et al., 2006; Cetin and Isik, 2007; Robertson, 2008). The contours of stress exponent suggested by Cetin and Isik (2007) are very similar to those first suggested by Robertson and Wride (1998), updated by Zhang et al. (2002) and further modified slightly by Robertson (2008). The contours by Moss et al. (2006) are similar to those first suggested by Olsen and Malone (1988). The normalization suggested by Boulanger and Idriss (2004a) only applies to sands

where the stress exponent varies with relative density with a value of around 0.8 in loose sands and 0.3 in dense sands. Figure 2 shows a comparison of the stress exponent contours suggested by Robertson (2008) for $\sigma'_{vo}/p_a = 1.0$, Moss et al. (2006), and Boulanger and Idriss (2004a) on the normalized SBTn chart of $Q_{tn} - F_r$. The regions where the three methods provide similar values are highlighted and show that the methods agree on or close to the normally consolidated zone suggested by Robertson (1990). Wroth (1984) showed that the stress exponent is 1.0 for clays based on Critical State Soil Mechanics (CSSM) theory, which is reflected in the Robertson (1990 & 2008) contours. The contours suggested by Olsen and Malone (1988) and Moss et al. (2006) are not supported by CSSM.

Robertson (1990) stated that the soil behaviour type charts are global in nature and should be used as a guide for defining Soil Behaviour Type (SBT). Caution should be used when comparing CPT-based SBT to samples with traditional classification systems based only on grain size distribution and plasticity. Factors such as changes in stress history, in-situ stresses, macro fabric, cementation, sensitivity and void ratio/water content will also influence the CPT response and resulting SBT. The rate and manner in which the excess pore pressures dissipate during a pause in the cone penetration can significantly aid in identifying soil type.

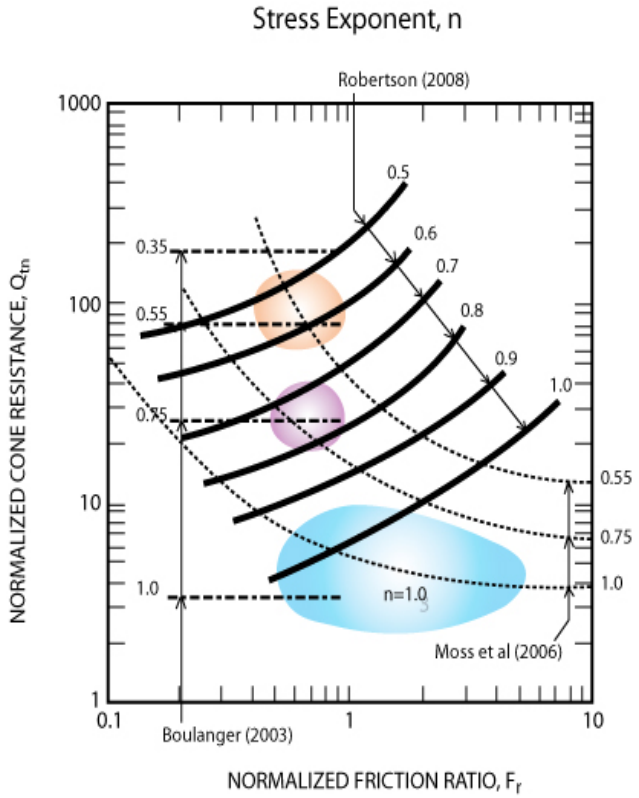

Figure 2. Comparison of contours of stress exponent 'n' on normalized SBTn chart $Q_{tn} - F_r$

Robertson (1990) and others have suggested that soils that have a SBTn index $I_c < 2.5$ are generally cohesionless where the cone penetration is generally drained and soils that have $I_c > 2.7$ are generally cohesive where the cone penetration is generally undrained. Cone penetration in soils with $2.5 < I_c < 2.7$ is often partially drained.

5 SOIL STRATIGRAPHY – TRANSITION ZONES

Robertson and Campanella (1983) discussed how the cone tip resistance is influenced by the soil ahead and behind the cone tip. Ahmadi and Robertson (2005) illustrated this using numerical analyses and confirmed that the cone can sense a soil interface up to 15 cone diameters ahead and behind, depending on the strength/stiffness of the soil and the in-situ effective stresses. In strong/stiff soils, the zone of influence is large (up to 15 cone diameters), whereas, in soft soils, the zone of influence is rather small (as small as 1 cone diameter). Ahmadi and Robertson (2005) showed that the zone of influence decreased with increasing stress (e.g. dense sands behave more like loose sands at high values of effective stress).

For interbedded soil deposits, the thinnest stiff soil layer for which the measured cone resistance represents a full response is about 10 to 30 cone diameters. Hence, as described by Robertson and Campanella (1983), soil parameters may be underestimated in thin stiff layers embedded within a softer soil (e.g. thin sand layers in a softer clay). Fortunately, the cone can sense a thin soft soil layer more precisely than a thin stiff soil layer. The fact that the cone can underestimate the soil resistance in thin stiff layers has led to the thin layer correction for liquefaction analyses (Robertson and Wride, 1998, Youd et al., 2001).

The zone of influence ahead and behind a cone during penetration will influence the cone resistance at any interface (boundary) between two soil types of significantly different strength and stiffness. Hence, it is often important to identify transitions between different soils types to avoid possible misinterpretation. This issue has become increasingly important with software (or spreadsheets) that provide interpretation of every data point from the CPT. When CPT data are collected at close intervals (typically every 20 to 50mm) several data points are 'in transition' when the cone passes an interface between two different soil types (e.g. from sand to clay and vice-versa). For thin stiff layers the two inter-

face regions can join such that the cone resistance may not represent the true value of the thin layer.

It is possible to identify the transition from one soil type to another using the rate of change of either I_c or Q_{tn}. When the CPT is in transition from sand to clay, the SBTn I_c will move from low values in the sand to higher values in the clay. Robertson and Wride (1998) suggested that the approximate boundary between sand-like and clay-like behaviour is around $I_c = 2.60$. Hence, when the rate of change of I_c is rapid and is crossing the boundary defined by $I_c = 2.60$, the cone is likely in transition from a sand-like to clay-like soil, or vice-versa. Profiles of I_c provide a simple means to identify these transition zones. Figure 3 illustrates a CPT profile through a deposit of interbedded sands and clays and shows how computer software (CLiq, 2008) can identify transition zones on the I_c profile based on the rate of change of I_c as I_c crosses the value 2.60. There are clear transitions from clay to sand (and vice-versa) at depths of 4.5, 8.5, 12.5, 14.1, 14.5, 16.9, 17.5, and 20.5m. The region between 5.0 to 8.0m, and again between 20.5 to 21.8m, represent soils close to the boundary of $I_c = 2.60$. Although these transitions could be identified from combinations of Q_{tn}, F_r and B_q, the algorithm (software) that identifies the zones on the profile of I_c appears to be more effective. Figure 3 also illustrates that the pore pressure measurements are less effective at shallow depths where saturation of the CPT sensor may be less effective. At depths of about 14m, 17m and 21m there are thin sand layers where the maximum values in the sand are likely too low due to the adjacent transition zones. Hence, identification of transition zones aids in the recognition of thin layers that may require correction (Youd et al., 2001).

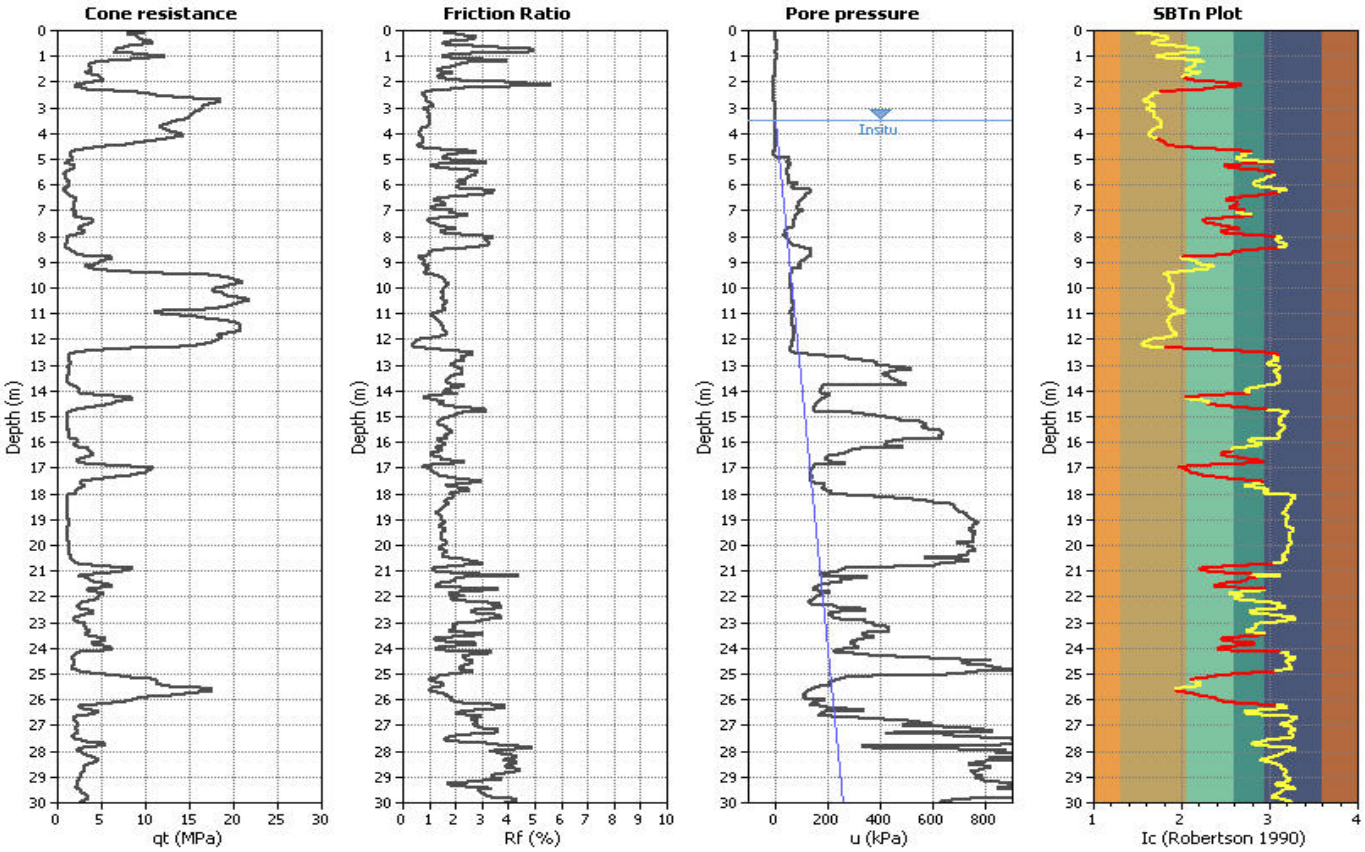

Figure 3. Example of interbedded soil profile with transition zones identified (in red) on SBTn I_c plot (CLiq Software, Geologismiki)

6 RESISTANCE TO EARTHQUAKE LOADING

Idriss and Boulanger (2008) present a summary of the history and background on the evaluation of liquefaction resistance to earthquake loading. They describe in detail how the Factor of Safety (FS_{liq}) against triggering of liquefaction in sand-like soils can be computed as the ratio of the soils CRR to the earthquake-induced CSR, with both the CRR and CSR values pertaining to the design earthquake magnitude (M) and in-situ effective overburden stress (σ'_{vo}):

$$FS_{liq} = CRR_{M,\sigma'_{vo}} / CSR_{M,\sigma'_{vo}} \quad (7)$$

Alternately, it is common to convert the earthquake-induced CSR into the reference condition applicable to M = 7.5 and σ'_{vo} = 1 atm. (i.e. σ'_{vo}/p_a = 1).

$$FS_{liq} = CRR_{M=7.5,\ \sigma'_{vo}=1} / CSR_{M=7.5,\ \sigma'_{vo}=1} \quad (8)$$

where:

$CRR_{M=7.5,\ \sigma'_{vo}=1}$ = Cyclic Resistance Ratio applicable to M = 7.5 and an effective overburden stress of σ'_{vo} = 1 atm., sometimes presented as simply $CRR_{7.5}$.

$CSR_{M=7.5,\ \sigma'_{vo}=1}$ = earthquake induced Cyclic Stress Ratio adjusted to the equivalent CSR for the reference values of M = 7.5 and an effective overburden stress of σ'_{vo} = 1 atm., sometimes presented as simply $CSR_{7.5}$.

For low-risk projects, CSR is typically estimated using the Simplified Procedure first described by Seed and Idriss (1971), using:

$$CSR_{7.5} = 0.65[a_{max}/g][\sigma_{vo}/\sigma'_{vo}]\ r_d\ [1/MSF][1/K_\sigma] \quad (9)$$

Alternate methods have been suggested for estimating the correction factors, r_d, MSF and K_σ.

Boundary lines have been developed that separate case histories in which 'liquefaction' was observed, from case histories in which liquefaction was not observed. This boundary line is used to provide the relationship between in-situ $CRR_{7.5}$ and an in-situ test index. Due to space limitations, this paper will only present CPT-based methods to estimate $CRR_{7.5}$.

6.1 *Sand-like (cohesionless) Soils*

$CRR_{7.5}$ for sand-like soils is generally defined in terms of 'triggering' liquefaction (i.e. reaching zero effective stress) although laboratory testing often uses a critical shear strain level (e.g. γ = 3%). Triggering of 'liquefaction' in loose sands is the onset of large strains. Therefore, since $CRR_{7.5}$ is traditionally used to define 'liquefaction' it can also be used to define the onset of large deformations. If the factor of safety against 'liquefaction' is less than 1 (i.e. FS_{liq} < 1) shear strains can be large and tend to increase as the factor of safety decreases, especially for loose sands.

The evaluation of CRR has evolved primarily from case histories of past earthquakes. The earliest efforts began with attempts to use SPT data (Kishida, 1966, Seed et al, 1984). In the early 1980's efforts were made to use CPT data (Zhou, 1980; Robertson and Campanella, 1985). In 1996-97, a workshop by NCEER and NSF provided a summary and recommendations on SPT-, CPT-, and Vs-based correlations and procedures (Youd et al., 2001). Following the NCEER workshop several major earthquakes provided new case histories. Moss et al. (2006) produced a compilation of the expanded database.

The NCEER/NSF workshop provided a set of recommendations by over 20 leading experts and was summarized by Youd et al. (2001). Youd et al. (2001) recommended the Robertson and Wride (1998) method for the CPT-based approach to evaluate CRR for cohesionless soils (I_c < 2.60). However, since 1997 there have been several publications attempting to update these recommendations. These updates have led to some confusion in practice, since changes were suggested to both CSR and CRR, which often resulted in minor changes to the calculated FS_{liq}.

Traditionally, case history data have been compiled by identifying the combination of the earthquake-induced cyclic stress ratio, CSR, and in-situ test results that best represents the 'critical zone' where liquefaction was estimated to have occurred for each site. It has been common to adopt a magnitude M = 7.5 earthquake, an effective overburden stress of σ'_{vo} = 1 atm and case histories with modest static shear stress (i.e. essentially level ground conditions). The resulting $CSR_{7.5}$ values are plotted against the in-situ test results normalized to σ'_{vo} = 1 atm. The resulting plots are then used to develop boundary lines separating cases of 'liquefaction' from cases of 'non-liquefaction' and, therefore, a method to estimate the $CRR_{7.5}$. This paper will focus only on the approaches that use CPT results, since the CPT is generally considered more repeatable and reliable than the SPT and provides continuous data in a cost effective manner.

Although this traditional approach of using case history data has resulted in significant developments, the approach has some limitations. The following is a short description of the main limitations.

'Liquefaction' and 'Non-liquefaction': field evidence of 'liquefaction' generally consists of surface observations of sand boils, ground fissures or lateral spreading. Sites that show no surface features may have experienced either liquefaction or the development of significant pore pressures in some soil layers, but no sand boils resulted, either due to the depth of the layer or the overlying deposits. Also, sites that show no surface deformation features may have experienced significant pore pressure development in some soil layers, but showed limited post-earthquake deformations due to ground geometry and lack of any significant static loads. Few case

histories have well documented deformation records where deformations were recorded with depth.

Selecting the 'critical zone': the depth where 'liquefaction' was assumed to have occurred requires considerable judgment. Occasionally, this is based on linking sand boil material to a specific soil layer, but often the selection is more subjective.

Average data points to represent each site: considerable judgment is required to select an appropriate average value for the in-situ test. For SPT results this was simpler because there were often only 1 or 2 SPT values in the critical zone. However, for CPT results this is more difficult, since there can be many CPT values within a layer. CPT results often show that a soil layer is not uniform either in terms of consistency (i.e. density/state) or grain characteristics (e.g. fines content/plasticity). In critical soil layers, where the soil is non-uniform and the cone resistance is variable, an 'average' value can be misleading.

Although the SPT- and CPT-based design methods were developed using average values, the methods are generally applied to all data points for design. CPT data are generally recorded at 5cm depth intervals to provide a near continuous profile. Hence, application of case-history based design methods, using the near continuous CPT profile, incorporate some level of conservatism. Applying the CPT-based methods to average in-situ test values for design requires judgment in selecting appropriate representative average values, and details in the near continuous profile can be lost.

Although the traditional approach has limitations, it has resulted in relatively simply approaches to evaluate a complex problem. Moss et al. (2006) (based on Moss, 2003) compiled a comprehensive database based on CPT records. For this paper, the Moss (2003) database has been re-evaluated using the continuous digital CPT records, where available, to confirm or modify the estimated average in-situ test values. The re-evaluation focused primarily on case histories that plot close to the boundary lines, since these play a more important role in defining the boundary line. The near continuous CPT records were processed through software that incorporates the updated Robertson and Wride (1998); Zhang et al (2002) and Zhang et al. (2004) CPT-based method as well as transition zone detection and the updated Robertson (2008) stress normalization (equation 6) (CLiq www.geologismiki.gr). The re-evaluation showed that the Robertson and Wride (1998) method performed extremely well on the database of near continuous CPT records. Some sites that appeared to have 'liquefaction' average data points on the 'non-liquefaction' side of the boundary line actually predicted 'liquefaction' (i.e. had regions in the critical layer where the computed $FS_{liq} < 1$) when using the near continuous CPT data. Hence, at sites where the Robertson and Wride (1998) method would appear to have incorrectly predicted performance based on the case history results using Moss et al. (2006) average values, the method predicted the correct performance using the measured near continuous values in terms of liquefaction (i.e. $FS_{liq} < 1.0$) and post-earthquake deformations. Some key sites, where the average values selected by Moss et al (2006) were considered inappropriate, are the sites at Whiskey Springs (1983 Borah Peak earthquake). These sites were composed of gravelly sands to sandy gravels and the CPT results showed significant rapid variation caused by the gravel content. The CPT measurements at these sites were less reliable due to the gravel content, and the average values selected by Moss et al. (2006) were considered too high and unrepresentative of the loose sand matrix that likely dominated the buildup of pore pressures during the earthquake. Other key sites are Balboa Blvd. and Malden St. (1994 Northridge, USA) and Kornbloom (1982 Westmorland, USA). Average values can be misleading in interbedded soils and may not adequately represent the various individual soil layers.

Moss et al. (2006) and Juang et al. (2003) have used the expanded case history database based on average values to provide criteria based on probability. The re-evaluation, using near continuous CPT records, suggest some uncertainty on proposed levels of probability, due to the highly subjective nature of the average values selected and the observation that some 'liquefaction' and 'non-liquefaction' sites were incorrectly classified when using only the Moss et al. (2006) average values. It is recommended that the near continuous CPT data be used to evaluate various CPT-based liquefaction methods and not average values that were subjectively selected. It is also interesting to note that, to the authors knowledge, none of the more recent CPT-based methods (i.e. post-Youd et al., 2001) used the recorded near continuous CPT records from the case histories to confirm the accuracy of the proposed new methods.

The Moss et al. (2006) database included 182 case history results (146 'liq' and 36 'non-liq'). However, 30 cases (23 'liq' and 7 'non-liq') were described as 'Class C' data that were case histories where the CPT results were obtained using either 'non-standard or mechanical cone' or 'no friction sleeve data available'. The Class C data are clearly less reliable than the rest of the data, especially for methods that make use of the friction sleeve results in the form of either friction ratio, R_f (Moss et al.,

2006) or soil behavior type, I_c (Robertson and Wride, 1998; Juang et al., 2003). Robertson and Campanella (1983) showed that mechanical cone friction sleeve values can be significantly different from standard electric cone values in the same soil.

The database, (with Class C data removed) where liquefaction was observed, had earthquake magnitudes in the range $5.9 < M_w < 7.7$ and vertical effective stress in the range $15 \text{ kPa} < \sigma'_v < 135 \text{ kPa}$. The average vertical effective stress in the liquefied layers was 60 kPa. No liquefaction, based on surface observations, was considered to have occurred at a depth greater than 16m. The average depth for the critical liquefiable layers was around 5 to 6m.

All the CPT-based methods (to determine $CSR_{7.5}$) typically include corrections for depth (r_d), magnitude scaling factors (MSF) and overburden correction factor (K_σ). The variations in these correction factors when applied to the database are generally small. Hence, the database is insufficient to clarify which correction methods are appropriate for design. Most methods specify that consistency is required when applying the methods to design problems (i.e. use the same correction factors on which the method was based). This paper uses the correction factors (r_d, MSF, K_σ) suggested by the NCEER workshop (Youd et al., 2001), with $K_\sigma = 1.0$.

Figure 4 shows a summary plot of the re-evaluated expanded database in terms of CPT results in the form of $CSR_{7.5}$ versus normalized cone resistance (Q_{tn}). The Class C data are not included in Figure 4. Figure 4 includes some case history data where the soil was not considered to be 'clean sand', however, the resulting boundary line is unaffected, because the 'liq' data in soils that are not 'clean sands' have lower cone resistance (i.e. located to the left of the boundary line). The resulting boundary line is often referred to as the 'clean sand' boundary line.

Figure 4 also shows some of the most recent published correlations superimposed over the updated database. The comparison in Figure 4 is not strictly correct, since the various published procedures include different normalization procedures for the CPT results. Fortunately, the differences, when applied to the case history data, are generally small (less than 20%), since all of the case history data are from sites where the range in vertical effective stress was small ($15 \text{ kPa} < \sigma'_v < 135 \text{ kPa}$). The various correlations are similar in the region of maximum data ($20 < Q_{tn} < 100$). When Q_{tn} is larger than 100 the correlations differ, mainly due to the form of the suggested correlations. Hence, for 'clean sands' the baseline correlation to estimate $CRR_{7.5}$ from CPT results is reasonably well established, especially in the region defined by $20 < Q_{tn} < 100$. It is likely that there will be little gained from further evaluation of current case history data using average values for clean sands in the form of $CSR_{7.5} - Q_{tn}$ plots. It is also recommended that further fine-tuning of the $CRR_{7.5}$ relationships using average values will be ineffective, since the location of the boundary is sensitive to the judgment used to select appropriate average in-situ test values. The form of the relationship controls $CRR_{7.5}$ for $Q_{tn} > 100$, since very little field data exists in this range. The form of the relationship becomes important when the method is extended to estimate post earthquake displacements.

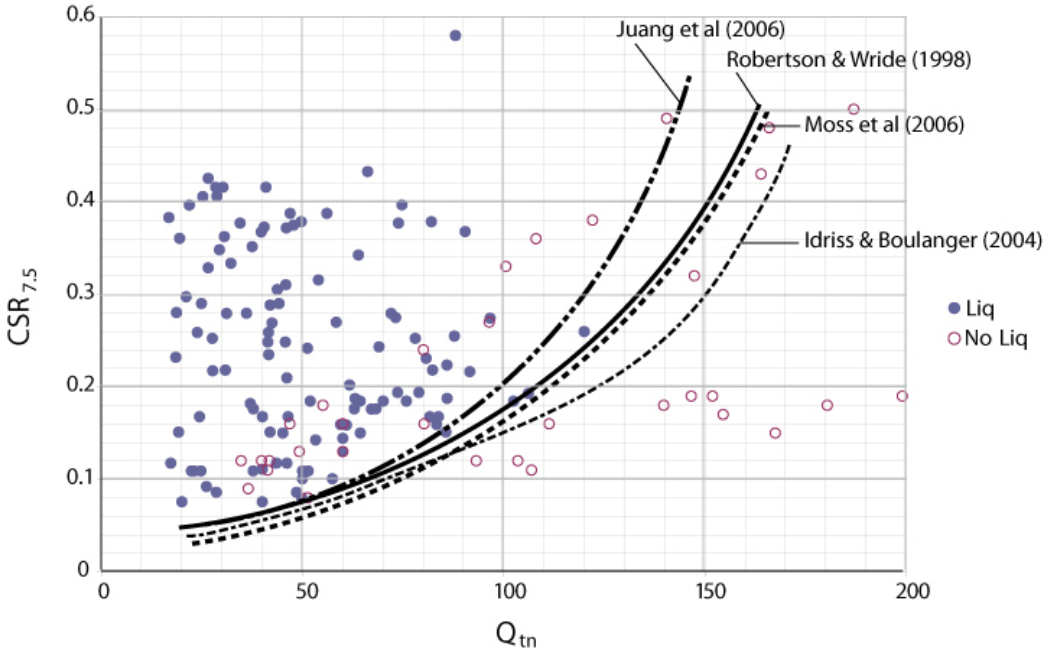

Figure 4. Updated case history database in terms of $CSR_{M=7.5,\square'vo=1}$ vs Q_{tn} (Class C data excluded)

For soils that are not 'clean sands', the traditional approach has been to adjust the in-situ penetration results to an 'equivalent clean sand' value. This evolved from the SPT-based approach where samples could be obtained and the easiest parameter to quantify changes in grain characteristics was the percent fines content.

Research has clearly shown that fines content alone does not adequately capture the change in soil behavior. Also, the average fines content of an SPT sample may not always reflect the variation in grain characteristics in heterogeneous soils, since it is common to place the full SPT sample into a container for subsequent grain size analyses, with resulting misleading 'average' fines content. The recent Idriss and Boulanger (2008) CPT-based approach that uses only fines content from samples to make adjustments to cone resistance is a retrograde step and is not recommended.

Several recent CPT-based liquefaction methods use modified CPT results to estimate clean sand equivalent values based on either SBT I_c (e.g. Robertson and Wride, 1998; Juang et al., 2006) or friction ratio, R_f, (Moss et al., 2006). Figure 5 shows a summary plot of the reevaluated expanded database, in terms of CPT results in the form of $CSR_{7.5}$ versus normalized clean sand equivalent cone resistance ($Q_{tn,cs}$), based on the corrections suggested by Robertson and Wride (1998) using I_c. Good agreement exists between the expanded database and the original Robertson and Wride (1998) CPT-based method.

Figures 6 and 7 show the updated database plotted on the normalized SBTn chart ($Q_{tn} - F_r$), where Q_{tn} and F_r were calculated using the method suggested by Zhang et al. (2002) and recently modified slightly by Robertson (2008). Figure 6 shows the case history data where $0.20 < CSR_{7.5} < 0.50$. Figure 7 shows the data where $CSR_{7.5} < 0.20$. The case history database is insufficient to subdivide the data into smaller divisions in the $Q_{tn} - F_r$ format, since both are on log scales. Presenting the case history data, in terms of the full CPT data (Q_{tn} and F_r) on the SBT chart, provides a different view of the influence of changing soil type on the correlations. Superimposed on the SBTn chart are the contours for $CRR_{7.5}$ suggested by Robertson and Wride (1998) in the region where $I_c < 2.60$. The Class C data are also included in Figures 6 and 7 but are identified using a different symbol. The Moss et al. (2006) corrections using friction ratio (R_f), appear to be influenced by the questionable Class C data. It is also interesting to note that, excluding the questionable Class C data, there are no case histories of observed 'liquefaction' based on average CPT values where $I_c > 2.60$. It is useful to remember that each data point, in terms of Q_{tn} and F_r, represents an average value for the critical layer.

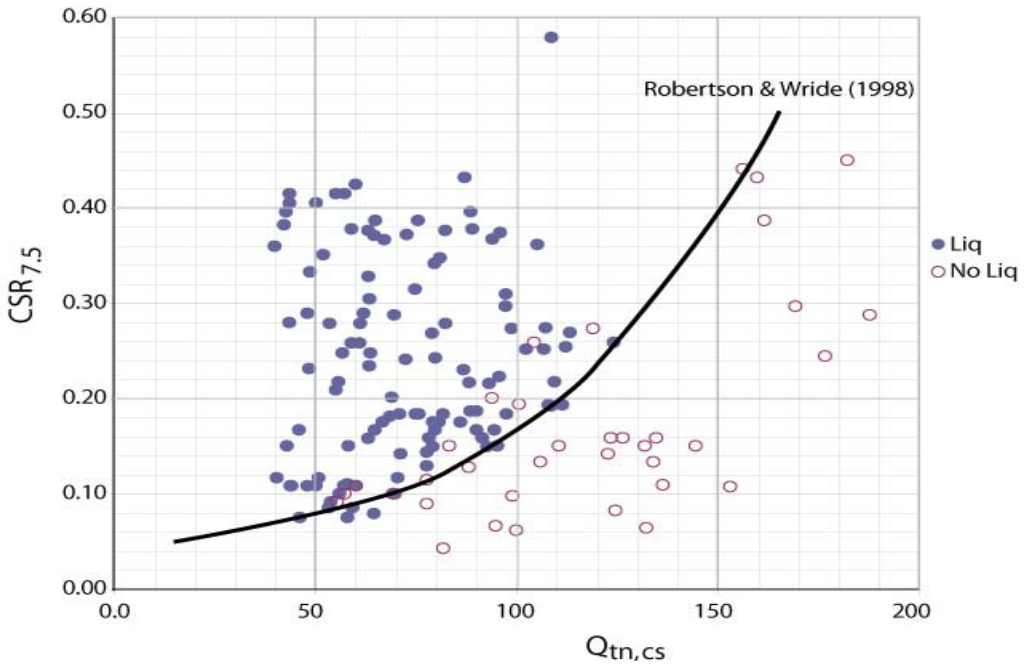

Figure 5. Updated case history database in terms of $CSR_{M=7.5,\square'vo=1}$ vs $Q_{tn,cs}$ (Class C data excluded)

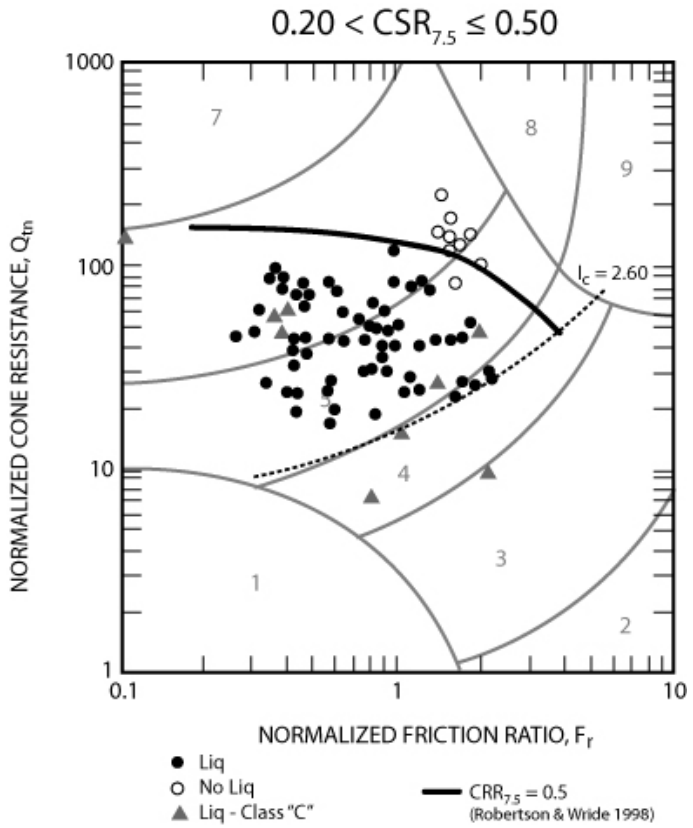

Figure 6. Updated database on SBTn $Q_{tn} - F_r$ chart for $0.20 < CRR_{7.5} < 0.50$ and Robertson and Wride (1998) contour for $CRR_{7.5} = 0.50$ ($I_c < 2.60$)

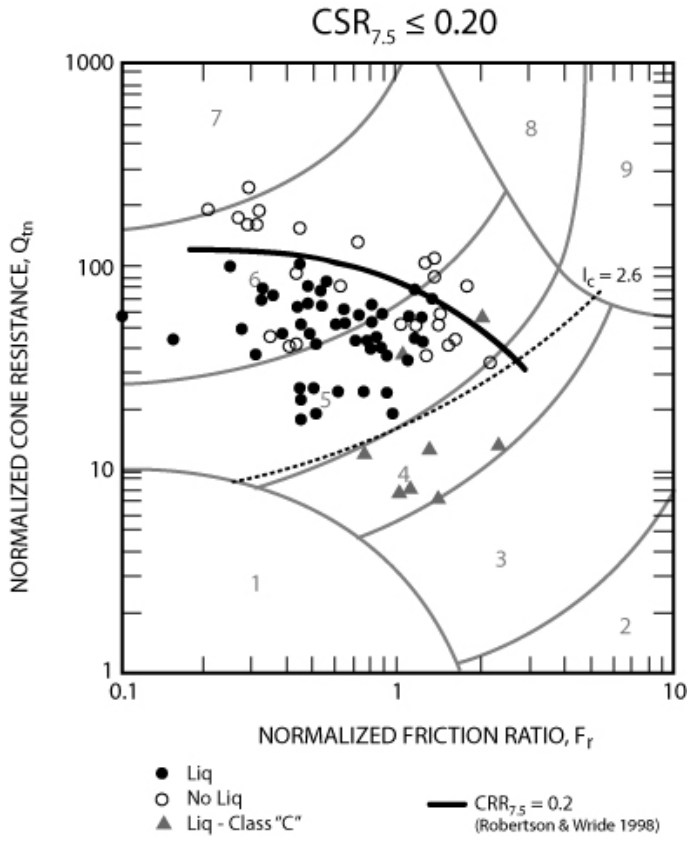

Figure 7. Updated database on SBTn $Q_{tn} - F_r$ chart for $CRR_{7.5} < 0.20$ and Robertson and Wride (1998) contour for $CRR_{7.5} = 0.20$ ($I_c < 2.60$)

Figure 8 shows the data where $CSR_{7.5} < 0.20$ with the correlations suggested by Olsen and Koester (1995); Suzuki et al. (1995); Robertson and Wride (1998) and Moss et al. (2006), for comparison. This format provides a way to compare the different 'correction' factors to adjust CPT results for soil type. The correlations suggested by Moss et al. (2006) appear to be too conservative at high values of either friction ratio or I_c. This was partly a result of using the unreliable Class C data, as well as inappropriate average values for some key sites, especially the sites from Whiskey Springs. The correlations suggested by Suzuki et al. (1995) and Olsen and Koester (1995) appear to be unconservative at high values of I_c, which was also pointed out by Robertson and Wride (1998).

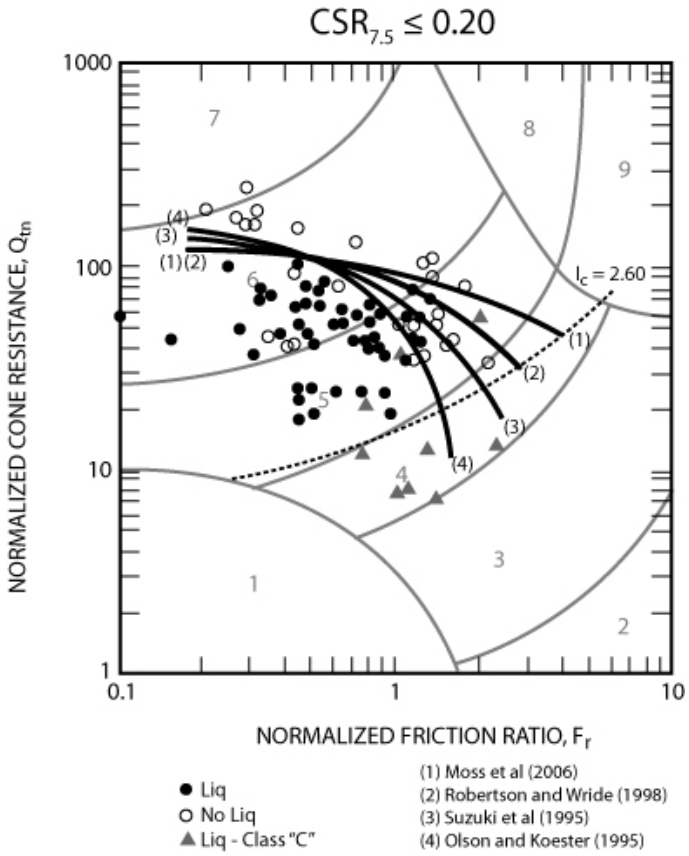

Figure 8. Comparison of published correlations on SBTn $Q_{tn} - F_r$ chart for $CRR_{7.5} < 0.20$

6.2 *Clay-like (cohesive) Soils*

Since cohesive clay-like soils are not susceptible to 'liquefaction', the criteria used to define CRR is deformation, which is often assumed to be a shear strain of $\gamma = 3\%$. Since detailed deformation records are uncommon in many case histories, much of our understanding regarding the response of cohesive soils to earthquake loading derives from undrained

cyclic laboratory testing. Fortunately, it is also possible to obtain high quality undisturbed samples in many clay-like soils.

Sangrey et al (1978) showed that fine-grained soils tend to reach a critical level of repeated loading that is about 80% of the undrained shear strength (s_u). Boulanger and Idriss (2006, 2007) provided a summary of the response of cohesive soils to cyclic loading. There is a strong link between the cyclic undrained response of fine-grained soils and their monotonic undrained response. The monotonic response of fine-grained soils is generally defined in terms of their peak undrained shear strength, s_u. Although the undrained shear strength is not a unique soil parameter, since it varies with the direction of loading, it does provide a simple way to understand the behavior of cohesive soils and captures many features (e.g. stress history, age and cementation). During earthquake loading, the predominant direction of loading is simple shear; hence, the undrained strength in simple shear is often the most appropriate parameter to link with CRR. Since earthquake loading is best defined in terms of CSR (τ_{cy}/σ'_v), it is appropriate to compare this with the undrained strength ratio (s_u/σ'_v). In simple terms, if the earthquake imposes a shear stress ratio that is close to the undrained strength ratio of the soil, the soil will deform. Since earthquake loading is rapid and cyclic, the resulting deformations may not constitute 'failure' (i.e. unlimited deformations). However, shear deformations can be large and tend to progress during the earthquake. Boulanger and Idriss (2004) used the term 'cyclic softening' to describe the progression of shear strains during cyclic undrained loading in fine-grained soils.

Boulanger and Idriss (2004b) presented published data that showed that, when the CSR ratio approaches about 80% of s_u/σ'_v, deformations tend to become large. Wijewickreme and Sanin (2007) showed that the $CRR_{(\gamma = 3\%)}$ in low plastic silts is also controlled by their peak undrained shear strength ratio (s_u/σ'_v). Although it is common to treat low plastic silts as 'sand-like', their CRR is controlled by their undrained strength ratio. Hence, soft low plastic silts tend to 'behave' similar to soft clays, where their response is controlled by the undrained strength ratio.

Boulanger and Idriss (2007) suggested that the $CRR_{7.5}$ (for a shear strain of 3%) could be estimated using either:

$$CRR_{7.5} = 0.8\ (s_u/\sigma'_{vo}) \tag{10}$$

or

$$CRR_{7.5} = 0.18\ (OCR)^{0.8} \tag{11}$$

Both methods are equivalent, since Ladd (1991) showed that:

$$s_u/\sigma'_{vo} = 0.22\ (OCR)^{0.8} \tag{12}$$

Boulanger and Idriss (2004b) suggested a further reduction factor (K_α) to $CRR_{7.5}$, based on the static shear stresses existing at the time of the earthquake. Therefore, the factor of safety against cyclic softening (3% shear strain), for cases in which the static shear stresses are small (i.e. $K_\alpha = 1.0$), can be expressed as:

$$FS_{\gamma=3\%} = CRR_M / CSR_M = CRR_{7.5} / CSR_{7.5} \tag{13}$$

Boulanger and Idriss (2007) showed that the MSF for clays is different than that for sands. They also showed that the $CRR_{7.5}$ of saturated clays and plastic silts can be estimated by three approaches:

- Directly measuring CRR by cyclic laboratory testing on undisturbed samples.
- Empirically estimating CRR based on s_u profile.
- Empirically estimating CRR based on consolidation stress history (i.e. OCR) profile.

Boulanger and Idriss (2007) described that the first approach provides the highest level of insight and confidence, whereas the second and third approaches use empirical approximations to gain economy. For low risk projects, the second and third approaches are often adequate. Based on the work of Wijewickreme and Sanin (2007) it would appear that the $CRR_{7.5}$ for soft low plastic silts can also be estimated using the same approach.

Robertson (2008) showed that CPT results in fine-grained soils are influenced primarily by both stress history (OCR) and soil sensitivity (S_t) and that the normalized cone resistance (Q_{tn}) is strongly influenced by OCR and almost unaffected by S_t, whereas, the normalized friction ratio (F_r) is strongly influenced by S_t and almost unaffected by OCR. Hence, Robertson (2008) suggested that the peak undrained shear strength ratio in cohesive soils can be estimated from:

$$(s_u/\sigma'_{vo}) = \left(\frac{q_t - \sigma_{vo}}{\sigma'_{vo}}\right)(1/N_{kt}) = Q_{tn} / N_{kt} \tag{14}$$

when $I_c > 2.60$ and $n \sim 1.0$)

where N_{kt} = empirical cone factor with an average value of 15.

Hence, when $K_\alpha = 1.0$:

$$CRR_{7.5} = 0.8\ Q_{tn} / 15 = 0.053\ Q_{tn} \quad (15)$$

Alternately, the OCR of clay can be estimated using (Kulhawy and Mayne, 1990):

$$OCR = 0.33\ Q_{tn} \quad (16)$$

Hence, when $K_\alpha = 1.0$:

$$CRR_{7.5} = 0.074\ (Q_{tn})^{0.8} \quad (17)$$

For values of $Q_{tn} < 10$ (i.e. $CRR_{7.5} < 0.5$), both approaches produce similar values of $CRR_{7.5}$.

Hence, estimates of $CRR_{7.5}$ can be made from CPT results using the normalized cone resistance Q_{tn}, since $CRR_{7.5}$ is controlled primarily by the peak undrained shear strength ratio. Note that in clays and silts where $I_c > 2.60$, $Q_{tn} = Q_{t1}$.

6.3 *All Soils:*

By combining the Robertson and Wride (1998) approach for cohesionless sand-like soils with the Boulanger and Idriss (2007) recommendations for cohesive clay-like soils, it is possible to provide a simple set of recommendations to estimate $CRR_{7.5}$ from CPT results for a wide range of soils.

The recommendations can be summarized, as follows:

When $I_c \leq 2.60$, assume soils are sand-like:

Use Robertson and Wride (1998) recommendation based on $Q_{tn,cs} = K_c\ Q_{tn}$, where K_c is a function of I_c. Robertson and Wride (1998) set a minimum level for $CRR_{7.5} = 0.05$.

When $I_c > 2.60$, assume soils are clay-like where:

$$CRR_{7.5} = 0.053\ Q_{tn}\ K_\alpha \quad (18)$$

Boulanger and Idriss (2007) suggested that, in clay-like soils, the minimum level for $CRR_{7.5} = 0.17\ K_\alpha$ for soft normally consolidated soils.

For a more continuous approach, it is possible to define a transition zone between sand- and clay-like soils:

When $I_c \leq 2.50$, assume soils are sand-like:
Use Robertson and Wride (1998) recommendation based on $Q_{tn,cs} = K_c\ Q_{tn}$, where K_c is a function of I_c.

When $I_c > 2.70$, assume soils are clay-like, where:

$$CRR_{7.5} = 0.053\ Q_{tn}\ K_\alpha \quad (19)$$

When $2.50 < I_c < 2.70$, transition region:
Use Robertson and Wride (1998) recommendations based on $Q_{tn,cs} = K_c\ Q_{tn}$, where:

$$K_c = 6x10^{-7}\ (I_c)^{16.76} \quad (20)$$

The recommendations where $2.50 < I_c < 2.70$ represent a transition from drained cone penetration to undrained cone penetration where the soils transition from predominately cohesionless to predominately cohesive.

Figures 9 and 10 show the proposed combined relationships for $CRR_{7.5} = 0.5$ and 0.2, respectively, compared to the expanded database. Additional non-liquefaction data points (28 in total) have been added from the published case history records. The 'non-liquefaction' points reflect soil layers (predominately clay-like soils) that did not 'liquefy' and did not show any observable/recorded deformations (i.e. no cyclic failure). As noted above, the criteria to define $CRR_{7.5}$ in clay is a shear strain of 3%. Figure 9 includes two data points (Yalova Harbour and Soccer Field sites, Kocaeli earthquake, Turkey, 1999) where cyclic softening may have occurred in the soft clay layer during earthquake shaking but no significant post-earthquake deformations within the clay layers were observed or noted. The lack of observed deformation in the clay layers at the two sites in Turkey may have been due to small static shear stresses at the depth of the clay. Figure 10 includes one data point from the Moss Landing site (Sandholt Rd., Loma Prieta, 1995) where a soft silty clay (Q_{tn} = 4 to 5, F_r = 3 to 4%) appears to have been close to cyclic failure and where a small amount of post earthquake lateral deformation (approximately γ = 0.5%) was observed from slope indicator measurements (Boulanger et al., 1995) and where the $CSR_{7.5}$ was about 0.25.

Data from three sites (Marina District, Treasure Island and Alameda) with deposits of soft, sensitive San Fransico (SF) young Bay Mud are also identified in Figure 10. These sites likely experienced a $CSR_{7.5}$ of about 0.15 during the Loma Prieta earthquake but showed no reported signs of deformations within the clay layer. This may have been, in part, due to the rather small static shear stress at these sites within the soft clay. The less reliable Class C data have not been included in Figures 9 and 10.

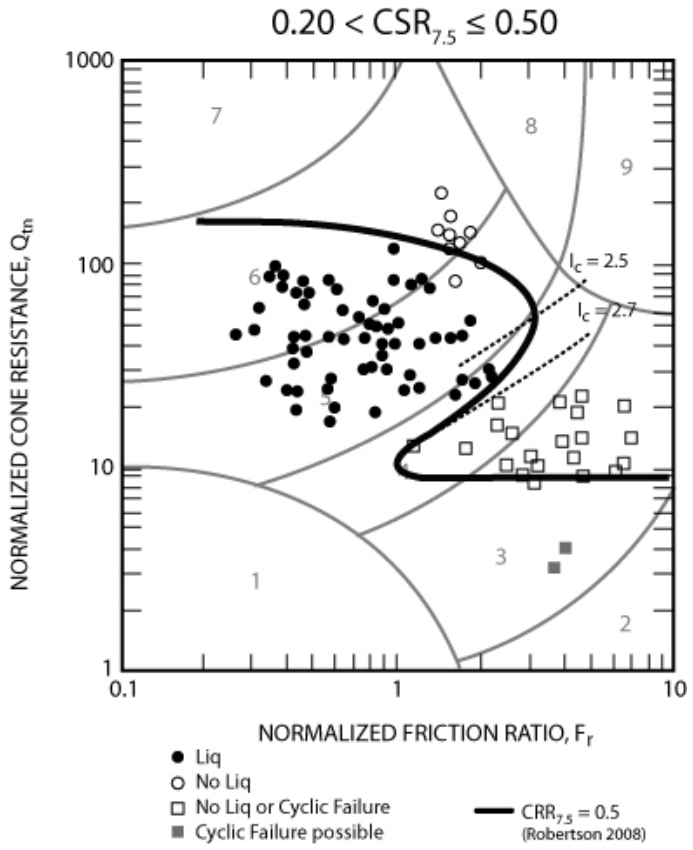

Figure 9. Proposed relationship to estimate $CRR_{7.5}$= 0.50 for a wide range of soils compared to updated database.

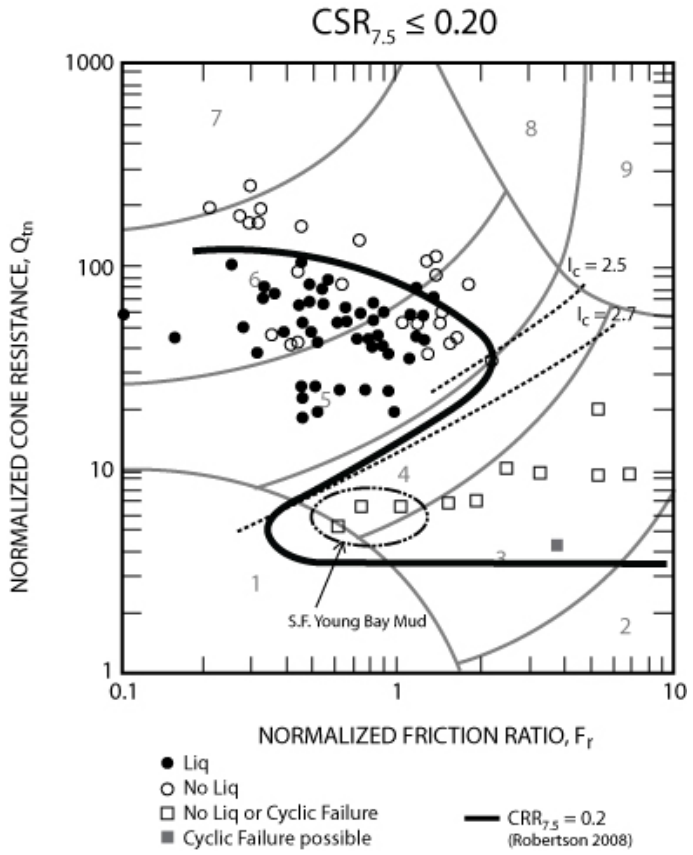

Figure 10. Proposed relationship to estimate $CRR_{7.5}$= 0.20 for a wide range of soils compared to updated database.

Boulanger and Idriss (2004) showed that high static shear stresses in soft clays can initiate cyclic failure during earthquake loading. They presented results from sites that experienced ground failure during the Kocaeli 1999 earthquake in soft clays where the static shear stresses were high. The above CPT-based approach to estimate CRR also correctly predicts ground failure at the sites presented by Boulanger and Idriss (2004) when $K_\alpha < 1.0$.

Typically, when $I_c > 2.60$ the soils are generally fine-grained and more easily sampled. Therefore, in this region ($I_c > 2.60$), selective sampling and laboratory testing can be appropriate, depending on the risk of the project.

7 POST EARTHQUAKE DEFORMATIONS

Estimating deformations in soils is generally difficult, due to the non-linear, stress dependent stress-strain response of soils. Estimating deformation after earthquake loading is more difficult, due in part to the complex nature of earthquake loading and the role of soil stratigraphy and variability.

Idriss and Boulanger (2008) present a summary of alternate approaches to estimating post earthquake deformations depending on the risk and scope of the project. For low to moderate risk projects it is common to estimate post-earthquake deformations by estimating strains and then integrate those strains over depth to estimate deformation. The estimated deformations may also be empirically adjusted on the basis of calibration to case history observations. For high risk projects it is appropriate to perform complex nonlinear dynamic numerical analyses if initial screening indicates a need.

7.1 *Vertical settlements due to reconsolidation*

Post-earthquake vertical displacements can develop in two ways: (1) settlement caused by reconsolidation, and (2) vertical displacement caused by shear deformation associated with lateral deformation. This section addresses only settlements caused by reconsolidation.

7.1.1 *Volumetric strains - cohesionless sand-like soils*

Post-earthquake reconsolidation volumetric strains are generally estimated using relationships derived primarily from laboratory studies. Methods are then evaluated using case history observations. One of the primary laboratory studies used is that by Ishihara and Yoshimime (1992) for cohesionless soils. Ishihara and Yoshimine (1992) observed that volu-

metric strains of sand samples were directly related to the maximum shear strain during undrained cyclic loading and to the initial relative density of the sand. Ishihara and Yoshimine (1992) showed that when $FS_{liq} > 1$ some shear and volumetric strains still occur and that as the FS_{liq} decreases ($FS_{liq} < 1$), shear and volumetric strains increase but reach maximum values depending on the relative density. When $FS_{liq} < 1.0$, loose cohesionless soils have reached zero effective stress with a loss of structure/fabric, the stiffness of the soil is then very small during reconsolidation that can result in large volumetric strains.

Zhang et al. (2002) coupled the Robertson and Wride (1998) CPT-based method using clean sand equivalent values to determine FS_{liq} with the Isihahara and Yoshimine (1992) volumetric strain relationships, to provide a method to estimate the post-earthquake vertical reconsolidation settlements. Zhang et al. (2002) evaluated the approach using case history observations and showed that the approach provided reasonable predictions of settlements, although details on site geometry and soil stratigraphy play an important role. Since most cohesionless soils have relatively high permeability, the post-earthquake reconsolidation settlements occur relatively soon after the earthquake, but depend on soil stratigraphy and drainage.

7.1.2 *Volumetric strains - cohesive clay-like soils*

Factors affecting vertical (1-D) settlement caused by post-earthquake reconsolidation of clay layers are discussed in Ohara and Matsuda (1988), Matsuda and Ohara (1991) and Fiegal et al. (1998). The limited laboratory data indicate that reconsolidation volumetric strains are controlled primarily by the max. shear strain which is function of the factor of safety ($FS_{\gamma=3\%}$) and stress history (OCR) of the soil. During undrained cyclic loading, pore pressures develop that result in a decrease in effective confining stress. However, the effective stresses generally do not reach zero and the soil retains some structure and stiffness. Wijewickreme and Sanin (2007) showed that, on average, for a wide range of fine-grained soils, when $FS_{liq} = 1$ the excess pore pressure represents about 80% of the effective confining stress (i.e. $\Delta u/\sigma'_{vo} = r_u = 0.8$). Volumetric strains occur as the soil reconsolidates back to the in-situ effective confining stress. The volumetric strains in cohesive soils during reconsolidation after earthquake loading are generally much smaller than those observed in cohesionless coarse-grained soils because cohesive soils retain some level of stiffness during reconsolidation. Case history field observations have also shown that post earthquake settlements, due to reconsolidation, are generally small at sites with thick deposits of cohesive soils. For example, the San Fransico Bay area in California has extensive thick deposits of soft (young) Bay Mud (essentially normally to lightly overconsolidated clay) but very few observations of measurable post-earthquake settlements within the clay deposits were made following the Loma Prieta earthquake. The re-evaluation of post-earthquake reconsolidation settlements at the Marina District, Treasure Island and Moss Landing sites following the Loma Prieta earthquake and sites in Taiwan following the Chi-Chi earthquake, suggest an average volumetric strain of less than 1% in fine-grained soils.

Volumetric strains for cohesive soils can be estimated using the 1-D constrained modulus, M, and the change in effective stress due to the earthquake loading where,

$$\varepsilon_{vol} = (\Delta\sigma'_v / M) \quad (21)$$

$$\Delta\sigma'_v = r_u \, \sigma'_{vo} \quad (22)$$

The buildup in pore pressure and hence, change in effective stress, is a function of the factor of safety (FS) and the OCR of the soil. Laboratory test results indicate that r_u is a function of FS. When FS = 1.0, $r_u = 0.8$ and when FS = 2, $r_u = 0$. Assuming a linear relationship between FS and r_u and an inverse relationship with OCR gives:

$$r_u = [0.8 - 2.66 \log (FS)]/OCR \quad (23)$$

where: r_u </= 1.0, when FS = 0.84

Kulhawy and Mayne (1990) showed that OCR can be estimated from the CPT using:

$$OCR = 0.33 \, Q_{tn} \quad (24)$$

Hence,

$$\Delta\sigma'_v = [0.8 - 2.66 \log (FS)] \, \sigma'_{vo} / 0.33 \, Q_{tn} \quad (25)$$

Assuming the 1-D constrained modulus during reconsolidation is generally larger than the initial constrained modulus estimated from the CPT:

$$M = A \, M_{CPT} \quad (26)$$

The 1-D constrained modulus estimated from the CPT is equivalent to the modulus from the in-situ stress to a higher stress, whereas during reconsolidation the cohesive soil has become overconsolidated due to the decrease in effective stress and the reconsolidation modulus is stiffer. For soft normally consolidated cohesive soils the reconsolidation stiffness is about 10 M_{CPT}. Whereas, in stiff overconsolidated

cohesive soils, the reconsolidation stiffness is approximately equal to M_{CPT}. Therefore, assume that *A* varies with OCR as follows:

$$A = 10 - 9 \log (OCR) \quad (27)$$

Since $OCR = 0.33\ Q_{tn}$

$$A = 10 - 9 \log (0.33\ Q_{tn}) \quad (28)$$

Robertson (2008) showed that in soft clays:

$$M_{CPT} = (Q_{tn})^2\ \sigma'_{vo} \quad (29)$$

Hence:

$$\varepsilon_{vol} = [0.8 - 2.66 \log (FS)]\ /\ [0.33\ A\ (Q_{tn})^3] \quad (30)$$

When $FS \leq 0.84$ set $r_u = 1.0$ & limit $\varepsilon_{vol} \leq 1\%$

The above procedure provides an approximate estimate of the post-earthquake reconsolidation volumetric strains in clay-like soils based on CPT results. The re-evaluation of the expanded case history database shows good agreement between observed post-earthquake settlements and those calculated using the Zhang et al. (2002) CPT-based method with the continuous CPT records incorporating the above method to estimate volumetric strains in clay-like soils.

7.2 *Lateral displacements due to shear deformation*

7.2.1 *Shear strains – Cohesionless soils*

Zhang et al. (2004) coupled the Robertson and Wride (1998) CPT-based method to determine FS_{liq} with the Isihahara and Yoshimine (1992) maximum shear strain relationships to provide a method to estimate the post-earthquake lateral displacement index (LDI). Zhang et al. (2004) used case history observations to modify the LDI based on ground geometry to estimate actual lateral displacements. Zhang et al. (2004) evaluated the approach using case history observations and showed that the approach provided reasonable predictions of settlements. Chu et al (2007) showed that the Zhang et al (2004) CPT-based method provided reasonable but generally conservative estimates of lateral displacements from the 1999 Chi-Chi (Taiwan) earthquake. Chu et al. (2007) also showed that shear strains at a depth more than twice the height of the free face should not be included in the method, since static shear stresses are likely too small to contribute to the lateral deformation.

7.2.2 *Shear strains – Cohesive soils*

The potential for shear deformations or instability in clay-like cohesive soils depends heavily on the static shear stresses (which can be captured via K_α) and the sensitivity of the soil.

Boulanger and Idriss (2004) have shown that high static shear stresses in soft clays can initiate high shear strains during earthquake loading. The CPT-based approach described here captures the decrease in FS in clay-like soils when an appropriate value of K_α is used.

If clays are sensitive and show significant strain softening in undrained shear (i.e. high sensitivity, S_t), strength loss can lead to significant deformations and instability. Boulanger and Idriss (2007) stated that the magnitude of strain, or ground deformation, that will reduce the clay's undrained shear strength (s_u) to its fully remolded value (s_{ur}) is currently difficult to assess, but it is generally recognized that it would require less deformation to remold very sensitive clays than more ductile relatively insensitive clays. Based on the assumption that the CPT sleeve friction (f_s) measures the remolded shear strength of the soil (i.e. $s_{ur} = f_s$), it is possible to estimate the sensitivity of clays using CPT results (Robertson, 2008); where:

$$S_t = s_u / s_{u(r)} = 7.1 / F_r \quad (31)$$

It is also possible to estimate the remolded undrained shear strength ratio (s_{ur} / σ'_{vo}) using (Robertson, 2008):

$$s_{ur} / \sigma'_{vo} = f_s / \sigma'_{vo} = (F_r \,.\, Q_{tn}) / 100 \quad (32)$$

As soil sensitivity increases, CPT data moves to the left on the $Q_{tn} - F_r$ SBTn chart, as F_r decreases with increasing S_t.

In a general sense, the $FS_{(\gamma=3\%)}$ is controlled by the OCR and peak undrained shear strength of the clay (i.e. Q_{tn}, equation 18) whereas the potential for strength loss and large deformations is controlled by the sensitivity of the clay (i.e. F_r, equation 31).

8 EVALUATION OF POST-EARTHQUAKE DEFORMATIONS USING CASE HISTORY OBSERVATIONS

Zhang et al. (2002; 2004) showed that CPT results could be used to provide reasonable estimates of post-earthquake reconsolidation settlements and lateral spread deformations. However, at that time there were limited case history records that had CPT

profiles. The earthquakes in Turkey and Taiwan in 1999 have now added to the case history records with CPT profiles and recorded deformations. The following is a brief summary of a comparison between shear deformations observed at sites in Taiwan and Turkey and those predicted using the Zhang et al. (2004) CPT-based method but with the updates described in this paper. Four sites experienced lateral spreading during the Kocaeli earthquake, Turkey in 1999, namely: Police Station, Soccer Field, Yalova Harbour and Degirmendere Nose sites. Several sites also experienced lateral spreading during the Chi-Chi earthquake in Taiwan in 1999. As noted earlier the sites at Yalova Harbour and Soccer Field have deposits of soft clay that would be predicted to have been close to cyclic failure, but appear to have had little influence on the lateral spread deformations due to the low static shear stress at the depth of the soft clay. Hence, these sites do not assist in our estimate of probable post-earthquake shear strains in clays. Figure 11 shows a summary of the predicted post-earthquake lateral displacements compared to the measured lateral displacements at the sites in Turkey and Taiwan based on the Zhang et al. (2004) CPT-based method with the updates described in this paper. The updated CPT-based method to estimate liquefaction and cyclic softening appears to provide reasonable estimates of lateral deformations.

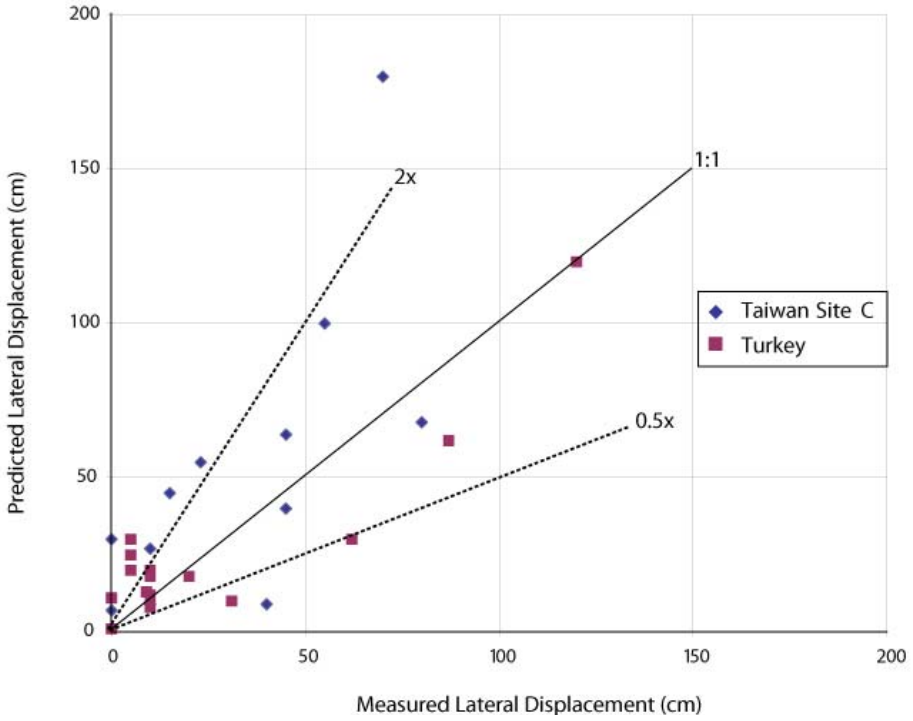

Figure 11 Measured post earthquake lateral displacements compared to predicted values using Zhang et al (2004) CPT-based method.

The updated CPT-based method, including the addition for estimating cyclic softening in clay-like soils, was used to re-evaluate the available case history CPT records and showed that clay-like soils generally play a minor role in almost all the available case history records. Although some clay-like soils likely experienced some cyclic softening during the earthquake, they generally appear to contribute little to the observed deformations, except the few cases where high static shear stresses contributed to ground failure (Boulanger and Idriss, 2004). In a general sense, cyclic softening and ground failure during seismic loading for clay-like soils is confined to soft, normally to lightly overconsolidated and/or sensitive fine-grained soils.

9 SUMMARY

This paper has presented an update of the Robertson and Wride (1998) CPT-based method to evaluate both liquefaction and cyclic softening in cohesionless and cohesive soils. Case history records have been carefully reviewed to re-evaluate the CPT-based method. Where possible, the near continuous CPT records have been used in the re-evaluation. The original Robertson and Wride (1998) method has been updated using a new stress normalization procedure that captures the change in soil response with increasing overburden stress and avoids the need for the K_σ correction for high overburden stresses. A transition zone detection feature has also

been included to identify zones where the near continuous CPT data may incorrectly interpret soil type, due to rapid variation at soil boundaries. The method has also been extended to include cohesive clay-like soils using the concepts described by Boulanger and Idriss (2004). The extension into the clay-like region avoids the need for a SBTn I_c cut-off to separate sand-like from clay-like soils.

Figure 12 presents a summary of the CPT SBTn $Q_{tn} - F_r$ chart to identify zones of potential liquefaction and/or cyclic softening. The chart in Figure 12 can be used as a guide for the choice of engineering procedures to be used in evaluating potential deformation and strength loss in different types of soils during earthquakes. Zones A_1 and A_2 correspond to cohesionless or sand-like soils for which it is appropriate to use existing CPT case-history based liquefaction correlations. Soils in Zones A_1 and A_2 are both susceptible to cyclic liquefaction, while the looser soils in zone A_2 are more susceptible to substantial strength loss. Zones B and C correspond to cohesive or clay-like soils for which it is more appropriate to use procedures similar to, or modified from, those used to evaluate the undrained shear strength of clays (e.g., field vane tests, CPT, and shear strength tests on high-quality thin-walled tube samples). Soils in Zones B and C are both susceptible to cyclic softening (e.g. accumulation of strains if the peak seismic stresses are sufficiently large), but the softer soils in Zone C are more sensitive and susceptible to potential strength loss. For moderate to high risk projects, undisturbed sampling of soils in Zones B and C is recommended to determine soil response, since soils in these zones are more suitable for conventional sampling and laboratory testing. Loose, saturated, non-plastic silts often fall in Zone C, however, their CRR is strongly controlled by undrained shear strength and the methods described for clay-like soils also apply. However, the resulting shear and volumetric strains should be evaluated based on either, undisturbed sampling and laboratory testing for moderate to high risk projects, or, assumed conservative values for low risk projects. For low risk projects, disturbed samples should be obtained for soils in Zones B and C to estimate if the soils will respond either more sand-like or clay-like, based on Atterberg Limits and water content.

The CPT is a powerful in-situ test that can provide continuous estimates of the potential for either liquefaction or cyclic softening and the resulting post-earthquake deformations in a wide range of soils. However, the CPT-based approach is a simplified method that should be used appropriately depending on the risk of the project. For low risk projects, the CPT-based method is appropriate when combined with selective samples to confirm soil type as well as conservative estimates of soil response. For moderate risk projects, the CPT-based method should be combined with appropriate additional in-situ testing, as well as selected undisturbed sampling and laboratory testing, to confirm soil response, where thin-walled tube sampling is generally limited to fine-grained soils in Zones B and C. For high risk projects, the CPT-based method should be used as an initial screening to indentify the extent and nature of potential problems, followed by additional in-situ testing and appropriate laboratory testing on high quality samples. Advanced numerical modeling is appropriate for high risk projects where initial screening indicates a need.

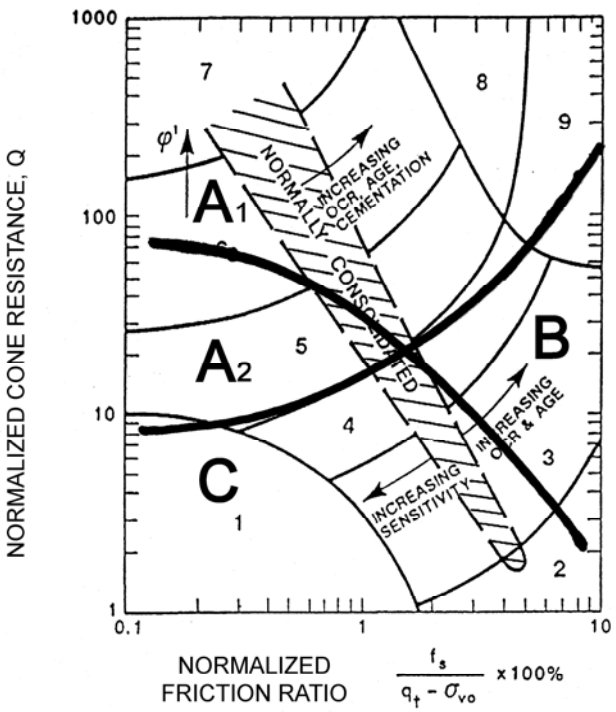

Figure 12. CPT Soil Behavior Type (SBTn) chart for liquefaction and cyclic softening potential:

Cohesionless soils (A_1 & A_2) - Evaluate potential behavior using CPT-based case-history liquefaction correlations.

A_1 Cyclic liquefaction possible depending on level and duration of cyclic loading.

A_2 Cyclic liquefaction and post earthquake strength loss possible depending on loading and ground geometry.

Cohesive soils (B & C) – Evaluate potential behavior based on in-situ or laboratory test measurements or estimates of monotonic and cyclic undrained shear strengths.

B Cyclic softening possible depending on level and duration of cyclic loading.

C Cyclic softening and post earthquake strength loss possible depending on soil sensitivity, loading and ground geometry.

10 ACKNOWLEDGMENTS

This research could not have been carried out without the support, encouragement and input from John Gregg, Kelly Cabal and other staff at Gregg Drilling and Testing Inc. Additional input and assistance was provided by John Ioannides.

11 REFERENCES

Ahmadi, M.M., and Robertson, P.K., 2005. Thin layer effects on the CPT qc measurement. *Canadian Geotechnical Journal*, **42**(9): 1302-1317.

Bray, J.D., and Sancio, R.B., 2006. Assessment of liquefaction susceptibility of fine-grained soils. *Journal of Geotechnical and Geoenvironmental Engineering,* ASCE, **132**(9): 1165-177.

Boulanger, R.W., Idriss, I.M., and Mejia, L.H., 1995. Investigation and Evaluation of Liquefaction Related ground displacements at Moss landing during 1989 Loma Prieta Earthquake. *Report No. UCD/CGM-95/02.* Center for Geotechnical Modeling, Department of Civil and Environmental Engineering, University of California, Davis.

Boulanger, R.W. and Idriss, I.M., 2004a. State normalization of penetration resistance and the effect of overburden stress on liquefaction resistance. *Proceedings 11th International Conference on Soil Dynamics and Earthquake Engineering.* Berkely, 484-491.

Boulanger, R.W. and Idriss, I.M., 2004b. Evaluating the potential for liquefaction or cyclic failure of silts and clays. *Report no UCD/CGM-04/01,* Center for Geotechnical Modeling, Department of Civil and Environmental Engineering, University of California, Davis.

Boulanger, R.W. and Idriss, I.M., 2006. Liquefaction susceptibility criteria for silts and clays. *Journal of Geotechnical and Geoenvironmental Engineering,* ASCE, 132(11): 1413-426

Boulanger, R.W., and Idris, I.M., 2007. Evaluation of cyclic softening in silts and clays. *Journal of Geotechnical and Geoenvironmental Engineering,* ASCE, 133(6): 641-52.

Cetin, K.O. and Isik, N.S., 2007. Probabilistic assessment of stress normalization for CPT data. *Journal of Geotechnical and Geoenvironmental Engineering,* ASCE, Vol. 133(7) 887-897.

Chu, D.B., Stewart, J.P., Youd, T.L., and Chule, B.L., 2006. Liquefaction induced lateral spreading in near-fault regions during the 1999 Chi-Chi, Taiwan earthquake. *Journal of Geotechnical and Geoenvironmental Engineering,* ASCE, Vol. 132(12) 1549-565.

Douglas, B.J., and Olsen, R.S., 1981. Soil classification using electric cone penetrometer. *In* Proceedings of Symposium on Cone Penetration Testing and Experience, *Geotechnical Engineering Division,* ASCE. St. Louis, Missouri, October 1981, pp. 209-227.

FEMA 356. Federal Emergency Management Agency, Washington, DC, Nov., 2008.

Fiegal, G.L., Kutter, B.L., and Idriss, I.M., 1998. Earthquake-induced settlement of soft clay. *Proceedings Centrifuge 98.* Balkema, Rotterdam (1) 231-36.

CLiq, 2008, Geologismiki: Geotechnical liquefaction software at http://w.w.geologismiki.gr/

Hight, D., and Leroueil, S., 2003. Characterization of soils for engineering purposes. *Characterization and Engineering Properties of Natural Soils,* Vol.1, Swets and Sitlinger, Lisse, pp. 255-360.

Idriss, I.M. and Boulanger, R.W., 2004. Semi-empirical procedures for evaluating liquefaction potential during earthquakes. *Proceedings 11th International Conference on Soil Dynamics and Earthquake* Engineering. Berkeley, 32-56.

Idriss, I.M. and Boulanger, R.W., 2008. Soil Liquefaction During Earthquakes. Earthquake Engineering Research Institute. MNO-12.

Jefferies, M.G., and Davies, M.O, 1991. Soil Classification by the cone penetration test: discussion. *Canadian Geotechnical Journal,* **28**(1): 173-176.

Jefferies, M.G., and Davies, M.P., 1993. Use of CPTU to estimate equivalent SPT N_{60}. *Geotechnical Testing Journal,* ASTM, **16**(4): 458-468.

Juang, C.H., Yuan, H., Lee, D.H., and Lin, P.S., 2003. Simplified Cone Penetration Test-based Method for Evaluating Liquefaction Resistance of Soils. *Journal of Geotechnical and Geoenvironmental Engineering,* ASCE, Vol. 129(1) 66-80.

Kishida, H. 1966. Damage to reinforced concrete buildings in Niigata City and Special reference to foundation engineering. *Soils and Foundations.* Japanese Society of Soil Mechanics and Foundation Engineering, 6(1), 71-86.

Kulhawy, F.H., and Mayne, P.H., 1990. Manual on estimating soil properties for foundation design, *Report EL-6800 Electric Power Research Institute*, EPRI, August 1990.

Lacasse, S., and Nadim, F., 1998. Risk and reliability in geotechnical engineering. State-of-the-Art paper. *Proceedings of 4th International Conference on Case Histories in Geotechnical Engineering.* St. Louis, Missouri, Paper No. 50.A.-S.

Ladd, C.C., 1991. Stability evaluation during staged construction (22nd Terzaghi Lecture). *Journal of Geotechnical Engineering*, **117**(4):540-615

Lunne, T., Robertson, P.K., and Powell, J.J.M., 1997. *Cone penetration testing in geotechnical practice.* Blackie Academic, EF Spon/Routledge Publ., New York, 1997, 312 pp.

Matsuda, H. and Ohara, S., 1991. Settlement calculations of clay layers induced by earthquake. *Proceedings 2nd International Conference on Recent Advances in Geotechnical Earthquake Engineering and Soil Dynamics.* St. Louis, M.O. pp, 473-79.

Moss, R., 2003. CPT-based Probabilistic Assessment of Seismic Soil liquefaction initiation. PhD. Thesis. University of California, Berkeley.

Moss, R.E.S., Seed, R.B., and Olsen, R.S. 2006. Normalizing the CPT for overburden stress. *Journal of Geotechnical and Geoenvironmental Engineering,* **132**(3): 378-387.

NBC 2005. National Building Code of Canada. National Research Council Canada.

Ohara, S., and Matsuda, H., 1988. Study on the settlement of saturated clay layer induced by cyclic shear. *Soil and Foundations.* Japanese Society for Soil Mechanics and Foundation Engineering 28(3), 103-13.

Olsen, R.S., and Malone, P.G., 1988. Soil classification and site characterization using the cone penetrometer test. *Penetration Testing 1988*, ISOPT-1, Edited by De Ruiter, Balkema, Rotterdam, Vol.2, pp.887-893.

Olsen, R.S., and Koester, J.P. 1995. Prediction of liquefaction resistance using the CPT. *Proceedings of the International Symposium on Cone Penetration Testing,* Vol.2, Swedish Geotechnical Society, Linkoping, pp. 257-262.

Robertson, P.K., 1990. Soil classification using the cone penetration test. *Canadian Geotechnical Journal,* **27**(1): 151-158.

Robertson, P.K., 1998. Risk-based site investigation. *Geotechnical News*: 45-47, September 1998.

Robertson, P.K., 2008. Interpretation of the CPT: a unified approach. Manuscript submitted to the *Canadian Geotechnical Journal*.

Robertson, P.K., and Campanella, R.G., 1983. Interpretation of cone penetration tests – Part I (sand). *Canadian Geotechnical Journal*, **20**(4): 718-733.

Robertson, P.K. and Campanella, R.G., 1985. Liquefaction Potential of sands using the cone penetration test. *Journal of Geotechnical Engineering Division,* ASCE, **111**(3): 384-406.

Robertson, P.K. and Wride, C.E., 1998. Evaluating cyclic liquefaction potential using the cone penetration test. *Canadian Geotechnical Journal*, Ottawa, **35**(3): 442-459.

Robertson, P.K., Campanella, R.G., Gillespie, D., and Rice, A., 1986. Seismic CPT to measure in-situ shear wave velocity. *Journal of Geotechnical Engineering Division,* ASCE, **112**(8): 791-803.

Sangrey, D.A., Castro, G., Poulos, S.J., and France, J.W., 1978. Cyclic loading of sands, silts and clays. *Proceedings of ASCE Specialty Conference Earthquake Engineering and Soil Dynamics*, Pasadena, Vol. 2 836-851.

SEAOC 1995 VISION 2000. Structural Engineers Association of California (SEAOC).

Seed, H.B., Tokimatsu, K., Harder, L.F. Jr., and Chung, R., 1984. The influence of SPT Procedures on Soil Liquefaction Resistance Evaluation. *Report No. UCB/EERC-84/15,* Earthquake Engineering Research Center, University of California, Berkeley.

Seed, H.B., and Idriss, I.M., 1971. Simplified Procedure for evaluating soil liquefaction potential. *Journal Soil Mechanics and Foundations Div*., ASCE 97(SM9), 1249-273.

Seed, R.B., Cetin, K.O., Moss, R.E.S., Kammerer, A., Wu., J., Pestana, J., Riemer, M., Sancio, R.B., Bray, J.D., Kayen, R., and Faris, A., 2003. Recent advances in soil liquefaction engineering: a unified and consistent framework. Keynote presentation, *26th Annual ASCE Los Angeles Geotechnical Spring Seminar,* Long Beach, CA.

Suzuki, Y., Tokimatsu, K., Taya, Y., and Kubota, Y., 1995. Correlation between CPT data and dynamic properties of insitu frozen samples. *Proceedings 3rd International Conf. on Recent Advances in Geotechnical Earhquake Engineering and Soil Dynamics.* Vol. 1, St. Louis, M.O.

Wroth, C.P., 1984. The interpretation of in-situ soil tests. Rankine Lecture, *Geotechnique* (4).

Wijewickreme, D., and Sanin, M.V., 2007. Effect of Plasticity on the laboratory cyclic shear resistance of fine-grained soils. *Proceedings 4th International Conf. on Earthquake Geotechnical* Engineering, Thessaloniki, Greece.

Youd, T.L., Idriss, I.M., Andrus, R.D., Arango, I., Castro, G., Christian, J. T., Dobry, R., Finn, W.D.L., Harder, L. F., Hynes, M.E., Ishihara, K., Koester, J.P., Liao, S.S.C., Marcuson, W.F., Martin, G.R., Mitchell, J.K., Moriwaki, Y., Power, M.S., Robertson, P.K., Seed, R.B., and Stokoe, K.H., 2001. Liquefaction Resistance of soils: summary report from 1996 NCEER and 1998 NCEER/NSF workshop on evaluation of liquefaction resistance of soils. *J. Geotechnical and Geoenvironmental Eng.,* ASCE 127(10), 817-33.

Zhang, G., Robertson, P.K. and Brachman, R.W.I., 2002, Estimating Liquefaction induced Ground Settlements From CPT for Level Ground, *Canadian Geotechnical Journal,* 39(5): 1168-1180.

Zhang, G., Robertson, P.K. and Brachman, R.W.I., 2004. Estimating Liquefaction induced Lateral Displacements using the SPT or CPT. *J. Geotechnical and Geoenvironmental Eng.*, ASCE 130(8), 861-71.

Zhou, S., 1980. Evaluation of the liquefaction of sand by static cone penetration tests. *Proceedings 7th World Conference on Earthquake Engineering*, Istanbul, Turkey, Vol. 3, 156-162.